STRUCTURE OF THE EYE AND PHOTORECEPTORS OF THE NEMATODE *MERMIS NIGRESCENS*

by

Abir Ahmed Khalil Mohamed

B.Sc., Al-Azhar University, 1993

M.Sc., Al-Azhar University, 1998

THESIS SUBMITTED IN PARTIAL FULFILLMENT OF

THE REQUIREMENTS FOR THE DEGREE OF

MASTER OF SCIENCE

in the Department

of

Biological Sciences

SIMON FRASER UNIVERSITY

August 2003

APPROVAL

Name: Abir Ahmed Khalil Mohamed

Degree: Master of Science

Title of Thesis:

Structure of the eye and photoreceptors of the nematode *Mermis nigrescens*.

Examining Committee:

Chair: Dr. A.T. Beckenbach

Dr. A.H. Jay Burr, Associate Professor, Senior Supervisor
Department of Biological Sciences, S.F.U.

Dr. L.M. Quarmby, Associate Professor
Department of Biological Sciences, S.F.U.

Dr. I. Novales Flamarique, Assistant Professor
Department of Biological Sciences, S.F.U.

Dr. N. Hawkins, Assistant Professor
Department of Molecular Biology and Biochemistry, S.F.U.
Public Examiner

4 August 2003
Date Approved

PARTIAL COPYRIGHT LICENCE

I hereby grant to Simon Fraser University the right to lend my thesis, project or extended essay (the title of which is shown below) to users of the Simon Fraser University Library, and to make partial or single copies only for such users or in response to a request from the library of any other university, or other educational institution, on its own behalf or for one of its users. I further agree that permission for multiple copying of this work for scholarly purposes may be granted by me or the Dean of Graduate Studies. It is understood that copying or publication of this work for financial gain shall not be allowed without my written permission.

Title of Thesis/Project/Extended Essay

Structure of the eye and photoreceptors of the nematode *Mermis nigrescens*.

.

Author: _____
(signature)

_____
(name)

14 August 03
(date)

Abstract

Female *Mermis nigrescens* (Mermithidae, Nematoda) is unique in having a single ocellus consisting of shadowing pigment and a positive phototaxis that guides it towards upper vegetation. The location of the photoreceptors in this ocellus is unknown. Previous experiments on the phototaxis of *Mermis* have suggested that photoreceptors must be located within the ocellus. In light of these studies, my research objective was to locate sensory structures in the ocellus, to describe their morphology, and to compare them with other nmatode sensory structures in order to distinguish them as photoreceptors. Another objective was to investigate the occurrence of the photoreceptors in younger females that lack the shadowing pigment and have negative rather than positive phototaxis, namely immature females and fourth stage juveniles. Serial semi-thick and ultra-thin sections through the ocellus were examined by both light and transmission electron microscopy.

The pigmented structure extends from approximately 80 μm posterior to the tip to a length of about 250-300 μm with a diameter of 106 μm. It begins just anterior to where the cuticle thickens into a 'collar' and ends posterior to where the body wall muscle begins. Two amphidial and four cephalic nerve tracks pass longitudinally through the cylinder. In the collar region, lamellae are observed to project perpendicularly from one of the dendrites in each amphidial track and invaginate a sheath cell. Their location, approximately 20 μm posterior to the amphids and cephalic sensilla, within the pigment cylinder, and their non-ciliary structure distinguishes these presumed photoreceptor organelles from the chemoreceptor dendrites at the distal end of the amphidial tracks. In the immature female and fourth stage juvenile, a similar lamellar

structure projects into a sheath cell in each track at about the same longitudinal position.

The hypodermal cells in the adult female are packed with hemoglobin crystals that appear in transverse section as dense inclusions 0.3-1.0 μm in diameter. The nucleus is displaced to the cell's periphery. In J4 juveniles and immature females, the cytoplasm of the hypodermal cells has fewer dense inclusions with smaller size, 0.1-0.2 μm in diameter, and the nucleus has a more typical location in the center.

Acknowledgments

I would like to thank my senior supervisor, Dr. Jay Burr for his support and continuous guidance during my research. I also am grateful to members of my supervisory committee, Dr. Lynne Quarmby for her encouragement and technical advice, and Dr. Inigo Flamarique for his valuable feedback. I would also like to thank Dr. Margo Moore for her guidance and encouragement. I would like also to thank Dr. Elaine Humphrey and Garnet Martens at UBC Bio-image facilities, for their instruction and guidance on electron microscopy. Finally, I would like to thank my parents and my husband Mohamed for their moral support, encouragement and patience.

Table of Contents

List of Tables

List of Figures

Chapter 1
General Introduction

1.1 The nematode *Mermis nigrescens*

Mermis nigrescens (Mermithidae) is a terrestrial nematode found in North America, Europe, and Australia. *M. nigrescens* has a significant economic importance as a natural biological control agent for controlling grasshopper populations (Baker and Capinera, 1997). The parasitic stages absorb nutrients from their host and kill it during emergence. Similar to other Mermithids, the free-living stages do not feed and utilize instead the food stored in the trophosome.

The life cycle of *M. nigrescens* differs from that of other Mermithids in that the female emerges from the soil to lay its eggs on vegetation. The positive phototaxis could aid the female to move toward the sky and climb to upper vegetation (Burr et al., 1989). Light stimulates oviposition that occurs on vegetation where grasshoppers feed (Cobb, 1926, Ellenby, 1964).

Each egg of *Mermis* contains a fully developed infective juvenile that is released in the host's gut and passes into the hemocoel. In the hemocoel, the juvenile absorbs nutrients through the cuticle and stores the food in the trophosome (Rutherford and Webster, 1974). The parasite leaves its host as the fourth stage juvenile (J4) that is negatively phototactic. Negative phototaxis could help the nematodes to crawl towards the soil surface (Burr et al., 2000b). The immature female lies dormant in soil for two years while utilizing its trophosome and developing eggs.

1.1.1 Eye morphology and photobehavior

Adult female *M. nigrescens* has a single putative ocellus containing a cylindrical accumulation of crystalline oxyhemoglobin (Ellenby and Smith, 1966; Burr and Harosi, 1985; Burr et al., 2000a). The hemoglobin has a shadowing role in detecting the direction of light (Burr, 1989; Burr and Babinszki, 1990).

For monochromatic light in the wavelength range 420-500 nm, the female *Mermis* utilizes a unique scanning motion to orient towards the light source (Burr et al., 1989). The head (anterior ~2 mm) bends sideways and vertically, increasing the probability of discovering the light source. Also, the scanning motion is involved in maintaining the worm's orientation towards light. However, the orientation towards light is independent of head motion of the nematode (Burr et al., 1990). Analysis of the motion in the presence of an optical illusion, Burr and Babinszki (1990) showed that both the proprioceptive signals that indicate and cause the head bending, and the photoreceptor signals caused by shadowing, are involved in orienting towards light during phototaxis. The experiment predicted that the photoreceptor must be located inside the hollow cylinder of hemoglobin pigment.

1.2 Nematode anterior nervous system

In the anterior tip of most nematodes, there are four types of cuticular sensilla containing sensory receptors. The cuticular sensilla are: two lateral amphids, the most complex sense organs in nematodes, four cephalic sensilla, six inner labial sensilla, and six outer labial sensilla. The number of the labial sensilla varies among different

nematodes. For example, in the filarial nematode, *Onchocerca volvulus,* the labial sensilla are reduced to pattern of 4+4 inner and outer labial sensilla (Strote et al., 1996). However, in the Mermithid, *Gastromermis boopthorae* has a 3+3 pattern (Batson, 1978).

The common structure of all nematode sensilla consists of three cells: the dendritic process, the distal end of a bipolar neuron and two non-neuronal cells, the sheath and the socket cell. A channel is formed by both the sheath and socket cells, into which the dendritic processes formed from modified cilia project from the dendrites. The sensory cilium contains microtubules arranged longitudinal along the length of the process (Lee, 1974; Wright, 1980; Ashton et al., 1999; Jones, 2002). The cilia are exposed to the outer environment through a pore. The pores allow direct access of external stimulating molecules to the ciliary membrane where they can bind with specific receptor molecules. The most distal non-neural cell, the socket cell, attaches the sensillum to the outer cuticle. Its proximal end forms a tight junction with the other non-neural cell, the sheath cell.

The sheath cell secretes a mucous-like substance into the channel that regulates the ionic environment around the dendritic process, which contain receptor molecules. In the sheath cell, golgi apparatus and endoplasmic reticulum produce the glyco-protein substance (Wright, 1983). Also, the sheath cell contains secretory granules containing secretion that might have an essential role for the function of the sensory processes (Jones, 2002). A tight junction connects the base of the sheath cell with the sensory dendrite that may serve to isolate the channel from the intracellular space and maintain a unique environment within the channel. The sensory end of the dendrite connects posteriorly via a long

process with its cell body, which is located in the lateral ganglion and is connected by its axon via synapses to other neurons in the nerve ring.

From the structure, it could be inferred that when the sensillum is connected to the outer environment via a pore, it has a chemosensory function (Wright, 1983). On the other hand, when the tip of the cilium is covered by a thin cuticle forming a papilla and not exposed to the external environment, as for example the inner labial sensillum of *O. volvulus*, the sensillum could be mechanosensory (Strote et al., 1996). In *Hammerschmidtiella diesingi,* the role of its mechanosensory neurons is to allow the nematode to remain in its host gut avoiding expulsion with its host feces (Trett and Lee, 1981). The capability of nematode sense organs to respond to many different stimuli suggests a high adaptive ability (Jones, 2002).

1.2.1 The amphids

A pair of large sensilla, the amphids, found in all nematodes, contain several different types of sensory dendrites in addition to the sheath and socket cells that form the amphidial channel. The different types and morphology of the organelles have been described in detail by serial section reconstruction (Ward et al., 1975; Ashton, 1999; Li et al., 2000a). In *C. elegans,* each amphid contains 12 sensory dendrites. Eight extend single dendritic processes into the channel that is exposed to the external environment (Ward et al., 1975). Because two of the eight processes have double ends, the total number in the channel is ten. The three remaining dendrites known as the wing cells (AWA, AWB, and AWC) have flattened processes that penetrate into the sheath cell with their flattened lamellar processes. One of the 12 amphidial neurons

projects numerous microvilli or finger-like processes. The finger cell (AFD) also ends in the amphidial sheath cell instead of in the channel. The AFD dendrite leaves the channel and penetrates into the sheath cell with its sensory processes. The AFD sensory organelle, therefore, is not connected to the external environment. All the amphidial dendrites connect to their cell body located in two lateral ganglions.

The amphid of *Haemonchus contortus* is similar in structure to that in *C. elegans* (Li et al., 2000a). The structural differences between the amphidial neurons suggest that each neuron might have a specific function. The laser beam ablation technique has been used to identify the possible function of the amphidial neurons (Bargmann et al., 1993; Li et al., 2000b). For example, the role of the amphidial dendrites AWA, AWB, and AWC in *C. elegans* is to detect specific volatile attractants during chemotaxis (Bargmann et al., 1993). The role of the ASJ, a single amphidial dendrite, in *H. contortus,* as in *C. elegans,* is to control the development of the nematode. In *H. contortus,* ASJ detects the environmental changes when the larva reaches its host's lumen after being ingested, and stimulates its development (Ashton, 1999).

On the other hand, amphid morphology differs among nematode species in many ways including the number of dendrites, the number of cilia in the amphidial channel, the number of the microtubules inside the cilia, and the shape of the amphidial channel (Ward et al., 1975; Coomans, 1979). In addition, the amphidial dendrites vary in shape, location, and size with nematode age and sex (Li et al., 2001).

Nematodes also have internal sense organs such as the touch receptors that are located near the cuticle. In the *C. elegans* anterior body, three types of touch receptors were described (ALML, ALMR, and

AVM) (Chalfie and Au, 1989). The touch receptors have microtubules that consist of 15 protofilaments, unlike the usual 11 protofilaments. Mutations resulting in touch insensitivity proved the mechano-sensory function (Chalfie and Thomson, 1982; Chalfie and Au, 1989).

1.3 Nematode eyes and photoreceptor organelles

In nematodes, the photoreceptors are commonly located within two-lateral ocelli containing a dense, granular pigment. The function of the pigment in the ocellus is to cast a shadow on the photosensitive organelles and thus to give a directional sensitivity (Siddiqui and Viglierchio, 1970b, Burr and Webster, 1971; Burr and Burr, 1975; Burr et al., 1989). The chemical nature of the pigments in nematodes has also been investigated (Bollerup and Burr, 1979). The shadowing pigment in nematodes comes in three types: melanin pigment as in *Oncholaimus vesicarius* and *Deontostoma californicum* (Burr and Webster, 1971, Croll et al., 1972; Bollerup and Burr, 1979), the crystalline oxyhemoglobin as in *M. nigrescens* (Ellenby and Smith, 1966; Burr and Harosi, 1985), and non-granular type of unknown chemical composition in *Araeolaimus elegans* (Croll et al., 1975).

The structure of the ocellus varies among nematodes. Some nematode ocelli have a cup-shaped pigment structure associated with a transparent refractive lens such as *Diplolaimella dievengatensis* (Van de Velde and Coomans, 1988), and some have a pigment cup but lack a true lens such as *D. californicum* (Siddiqui and Viglierchio, 1970 b). Others have simply a shallow cup, e.g. *Chromadorina* sp. (Croll et al., 1972), or a pigment spot, e.g. *O. vesicarius* (Burr and Burr, 1975), or a spherical ocellus, as in *Seuratiella sp* (Bollerup and Burr, 1979).

The photoreceptors of only five species of nematodes, marine and aquatic, have been identified based on their ultra-structure to date. The putative light sensitive membranes appear either as a modified stack of lamella, or in one case, a cluster of modified cilia. *Oncholaimus vesicarius* has a type of photoreceptor unique among nematode species. The ciliary photoreceptors are located in the amphidial bulb (Burr and Burr, 1975). On the other hand, *Diplolaimella dievengatensis*, *Chromadorina bioculata, Dentostoma californicum,* and *Araeolaimus elegans* have the multilamellar type of photoreceptor organelle (Van de Velde and Coomans, 1988; Croll et al., 1972; Siddiqui and Viglierchio, 1970a,b; Croll et al., 1975).

A behavioral response to light has been reported in a few nematode species, for example, *C. bioculata* (Croll et al., 1972), *O. vesicarius* (Burr and Burr, 1975), *C. elegans* (Burr, 1985), and *M. nigrescens* (Burr, et al., 1989; Burr and Babinszki, 1990; Burr et al., 2000b). In some cases of soil, terrestrial, and parasitic nematodes where photo-behavior has been described, including *C. elegans* (Burr, 1985), it was found that those nematodes lack pigment spots and none of their photoreceptors have been identified.

1.4 Comparison of nematode photosensory structures with those of other animals and protista

Photoreceptors are found in organisms from the unicellular protista to multicellular animals such as invertebrates and vertebrates. The structure of the photoreceptors differs in vertebrates and non-vertebrates. The photoreceptor structure of all vertebrates is a modified cilium: the retinal rods and cones. In the non-vertebrate, the photoreceptors have greater variety in structure. Examples of non-

vertebrate photoreceptors are 1) the membrane adjacent to the eyespot in unicellular protista such as flagellated protozoans, 2) the multilamellar, microvillar or multiciliary organelles in the ocelli of flatworms, rotifers and nematodes (Burr 1984), and 3) the microvillar rhabdoms in ommatidia of crustaceans and mollusks (Wolken, 1986).

A common feature in the nematode and many other invertebrates is photoreceptors located adjacent to and shaded by pigment structures that cast a shadow on the photosensitive organelles and thereby give a directional sensitivity (Wolken, 1977; Burr, 1984; Burr et al., 1989).

In some invertebrates, photoreceptors have unique locations. For example, the giant clam *Tridacna gigas* have thousands of marginal photoreceptors that are sensitive to shadows (Fankboner, 1981). The light sensitive organelle is a region of the plasmalemma in *Chlamydomonas reinhardii* (Wolken, 1986). In *Euglena* (Euglenophyta), the light sensitive organelle is the paraflagellar swelling, located in the base of the flagellum (Wolken, 1977; Hegemann et al., 2001).

The photoreceptors can detect light because they contain light-absorbing molecules called the visual pigments. The visual pigments, which are proteins (opsins) covalently linked to a chromophore (retinal, the aldehyde of vitamin A), are embedded in a membrane (Pepe, 1999). Vertebrates are different from non-vertebrates in how the chromophore of the visual pigment is regenerated during phototransduction. In vertebrates, the chromophore is released from opsin and is replaced during a regeneration process in which opsin is incorporated into a new stack of membranes. However, in non-vertebrate, the chromophore remains attached and available for a fast photo-regeneration process (Arnheiter, 1998; Pepe, 1999).

1.5 Theories of evolution of photoreceptors

It is not certain when photoreceptors evolved. However, there are some theories suggesting possible evolutionary trends that are based on either the cellular or the molecular level.

At the cellular level, Richard Eakin (1982) proposed that the photoreceptors are divided into two main types: the ciliary and the rhabdomeric (microvillar) types. The ciliary type may have evolved from the ciliary membrane, and the rhabdomeric type may have evolved from the distal cell membrane. In addition, Eakin (1982) claimed that the ciliary photoreceptors are found only in deuterostomia (echinoderms, chordates), and the rhabdomeric photoreceptors are found only in protostomes (mollusks, annelids, arthropods, and platyhelminthes). These observations suggested to Eakin that the photoreceptors have evolved along two lines, i.e. are polyphyletic in origin (Eakin, 1968, 1972, 1982).

However, many contradictions to Eakin's hypothesis have been found. Evidence for the presence of both types of the photoreceptors not only in the same phyla but also in the same animal suggested to Vanfleteren (1982) that both types of photoreceptors have a common ancestor of ciliary type, i.e. photoreceptors have monophyletic origin. The difference between both types is quantitative not qualitative.

Burr (1984) argued that there must be two additional types of photoreceptors: a) the epigenous photoreceptors, i.e. growing on the surface, and b) the mixed photoreceptors, i.e. projections of microvillous from the ciliary membrane. The epigenous type is found in most nematodes and in the rotifera *Rhinoglena frontalis*. The epigenous

photoreceptors are different than the modified cilia (of ciliary photoreceptors) and modified microvilli (of rhabdomeric photoreceptors) in having lamellar projections from the apical cell membrane of the dendrite. Another type of photoreceptors is the mixed type. In Cnidaria and Hemichordata, the photoreceptors have microvillous projections from the ciliary membrane. It is assumed that both mixed and epigenous are cenogenic, newly occurring in a taxa.

At the molecular level, an example for the ancestry of photoreceptors based on opsins sequences has been postulated by (Deininger et al., 2000). Comparison of the DNA and amino acid sequences of opsins from different phyla show that all animal opsin sequences have evolved from a common ancient opsin sequence. Algal opsin sequences reflect the ancient opsin genes since they show similarity in structure to animal opsins, in particular to invertebrate opsin more than vertebrate opsin (Deininger et al., 2000). Further, Arnheiter (1998) suggested that the differences in the opsin gene sequences between invertebrates and vertebrates are due to how the chromophores regenerate differently after photoactivation.

1.6 Objectives of this thesis

Previous studies have demonstrated that *M. nigrescens* has a unique ocellus and photosensitive behavior. However, the location of photoreceptors in the ocellus has not been described, although there is strong behavioral evidence that it is located within the cylindrical pigmented structure (Burr and Babinszki, 1990).

In this thesis, a microscopic study was conducted to attempt to answer the following questions: 1) where are the potential sites of the

photoreceptors? What type of photoreceptor is present? How do the photoreceptors differ from the other nematode sensory structures? And how might the photoreceptors of *Mermis* have evolved? Another objective was to investigate the occurrence of the photoreceptors in younger females, immature female and fourth-stage juvenile, that lack the shadowing pigment and have negative rather than positive phototaxis.

In order to attempt to answer these questions, a series of transverse sections through the ocellus were obtained. These sections were analyzed using both light and transmission electron microscopy for evidence of possible photoreceptor structure.

Another goal of this research was to devise an optimal method for preparing the nematode *M. nigrescens* for ultra-structural study, in order to investigate the photoreceptor morphology. This was achieved by a) evaluating the effects of using supplements with glutaraldehyde, b) improving the penetration of the solvents using microwave radiation, and c) deleting osmication and replacing it with uranyl acetate fixation. The results obtained with the latter method are compared with those of Locke (1994), whose technique was used to preserve the fine cytoskeletal structure in insects.

Chapter 2
Materials and Methods

2.1 Specimen source and maintenance

In late May, adult females of *Mermis nigrescens* (Cobb, 1926) were collected in B.C after emerging from the soil in a rainy day and crawling on vegetation to lay their eggs. The worms were placed in plastic bags containing moist soil, and stored in the fridge at 10 °C as described in (Christie, 1937).

2.2 Raising juveniles, immature and mature females

To obtain juveniles and immature females and increase the supply of the mature females of *M. nigrescens*, desert locusts, *Schistocerca gregaria*, were fed about 25 eggs placed on a small piece of grass. The eggs were isolated from the mature females *M. nigrescens* by cutting anterior and posterior to the vulva and collecting the eggs on a filter paper moistened with distilled water. The eggs were stored moist in the fridge at 10 °C. The stored eggs were fecund for about 2-3 months. Mature eggs contain J2 juveniles that are released in the locust alimentary canal within 4-6 hours of ingestion (Craig and Webster, 1978). The juveniles penetrate the alimentary canal using their stylet and enter the hemocoel. *Mermis* grow to full size as J3s and emerge after 4-5 weeks as fourth stage juveniles. Because some of the J4s emerge from the locust anus during the infection period, a plastic container filled with sterilized moist soil was placed in the cage bottom to prevent the emerged juveniles from drying out. After 4-5 weeks of infection, the

remaining J4s were collected from the locust hemocoel after ventrally slitting the thorax and abdomen. The female juveniles were stored at 10 °C in plastic bags containing moist autoclaved soil. The J4s molt to immature adult females in 3-10 days and develop to mature adult females in one to two years. During the storage period, the nematodes were susceptible to predation and fungus infections, therefore the soil was autoclaved prior to use and changed once a month. The soil became toxic if autoclaved more than once. With these treatments, a number of worms survived and developed eggs within a year and a half in the laboratory.

For TEM study, female J4s on day one of emergence were fixed for serial sectioning and ultra-structural observation. The female juveniles were identified from the male by their larger body size, their vulva precursor in the middle of the body, and the absence of the male gonad precursor. Immature adult females 2-4 weeks of post emergence were used for developing methods for TEM. Immature females 5-6 months post emergence had developed faintly visible amounts of hemoglobin pigmentation in the ocellus. Females cultivated for a year had a fully developed ocellus. These "mature females", the 5-6 month immature females and the emergent J4s were investigated to locate photoreceptors in the ocellar region.

2.3 Preparation of specimens for TEM

A number of experiments will be described in Chapter 3 in which the fixation procedures and solutions were varied. The following methods were used throughout.

2.3.1 Pretreatments

Before fixation, the worms were washed several times for 5 minutes in half-concentrated M9 buffer (Sulston and Hodgkin, 1988) with the addition of about 50 µL per 100 ml of Tween 20. The M9/2 was osmotically neutral. The detergent was added to remove the waxy layer that covers the outer surface of the nematode cuticle in order to make it more permeable to the fixative and resin. After washing, the nematodes were anesthetized in 8% ethanol or 0.1 M of sodium azide in M9/2. The anesthetic was used prior to fixation to relax the muscles and thus to prevent bending. A bent head causes difficulties during sectioning and results in oblique rather than the desired transverse sections.

2.3.2 Permeabilization

A number of procedures were important to facilitate fixative penetration and resin infiltration into the head. Immediately after placing a 0.5 cm piece of the anterior into a drop of the aldehyde fixative, the head was severed posterior to the cephalic ganglion and anterior to the trophosome. While in the fixative several holes were made in the cuticle with a sharp needle both anterior and posterior to the ocellus, and 3-4 holes were made posterior to the cephalic ganglia. In smaller worms such as *Haemonchus contortus*, a laser micro-beam is used (Li et al., 2000a). To improve the speed of penetration through the cuticle, microwave radiation (Pelco, model 3450 polymerizing processor) was used during fixation, rinsing, dehydration, and resin infiltration and polymerization. Resin polymerization in the microwave gives faster and better results than the conventional method (Giammara, 1993). During polymerization,

specimens in the embedding mold were placed in a beaker and covered with distilled water. The beaker was exposed for microwave radiation at 500 W for an hour.

2.4 Basic fixation protocol for TEM

After cutting in glutaraldehyde fixative, the anterior tip containing the ocellus (about 500 μm) was transferred into an Eppendorf tube containing freshly prepared 2.5% glutaraldehyde in 0.05 M Na cacodylate buffer and 1 mM $CaCl_2$. The tube was exposed in the microwave under vacuum at 200 W for 4 minutes. Then, while still in the fixative the cuticle was poked (as described above) and left for an hour at room temperature. The worms were washed in 0.2 M cacodylate buffer several times under microwave radiation (100 W for 30 seconds). Thorough rinsing at this step is important to prevent the precipitation of osmium during the next step.

The worms were post-fixed in 2% OsO_4 under microwave radiation (as with aldehyde fixative). The worms were washed several times in distilled water and dehydrated in a graded alcohol series (50-100%) and twice in 100% acetone under microwave radiation (100 W for 30 second). Propylene oxide is not recommended with microwave treatment. The worms were infiltrated in graded series of 3:1, 2:1, 1:1, 1:2 (acetone: resin) and three changes in pure resin under microwave radiation (200 W for 6 minutes). The resin was Epon 812: 12.5g mixed with 6.5 g dodecenylsuccinic anhydirde (DDSA), 18 drops 2, 4, 6-Tridimethylamino methyl phenol (DMP), 6 g nadic methyl anhydride (NMA), 13 g nonenyl succinic anhydride (NSA), 5 g vinylcyclohexene dioxide (epoxide resin low viscocity ERL), and 3 g diglycidyl ether of polypropyleneglycol (DER).

Specimens were transferred into molds containing pure resin. The resin was polymerized at 60 °C overnight or under microwave radiation (500 W) at 90 °C for an hour.

2.5 Sectioning and Staining

Serial thin and thick sections were obtained using an ultramicrotome (Leica Ultracut T). Prior to sectioning, blocks were trimmed to have smooth faces with exactly parallel sides only a few microns away from the specimen in order to obtain uniform, straight, and long ribbons as described in (Hall, 1995).

A diamond knife was used to cut ultra-thin and semi-thick sections. Semi-thick sections about 0.5 μm in thickness were placed on microscope slides with a drop of distilled water. The slides were dried on the hot plates for few seconds and stained with 1% toluidine blue for 5 seconds.

Ultra-thin sections about 60 nm in thickness were cut into ribbons floating on distilled water in the knife trough. Ribbons were collected on slotted grids coated with Formvar and carbon. Formvar-coated grids were prepared by:

1) Dissolving 0.3 grams of Formvar powder in 100 ml of dichloroethane and stored in a dark colored bottle and in a dry place. Moist solvent results in holes in the Formvar film that affect its stability.
2) Formvar films were prepared by placing a clean glass slide into the solution for 40 seconds and separating the film from the slide into the surface of distilled water as described in (Hayat, 2000).

3) Placing the grids on the film, dull side downwards.
4) Before placing the sections on the coated grids, the Formvar films were checked for holes and correct thickness under a dissecting scope, and tested for stability under the TEM beam. In addition, to increase the stability, the grids were coated with carbon.

Ultra-thin sections were stained to obtain a higher contrast. Grids were immersed in a drop of 2% aqueous uranyl acetate for 10 minutes and rinsed for several times in distilled water. Then, they were stained for 5 minutes in a drop of lead citrate in a petri dish containing several NaOH pellets. Finally, the grids were rinsed in distilled water.

2.6 Microscopy

The transmission electron microscope (Hitachi H-7000, Hitachi, Ltd., Tokyo, Japan) was operated at an acceleration voltage of 80 kV and a 50 μm aperture to obtain high-resolution images of the ultra-thin sections. Photographs were taken digitally with the AMT Advantage HR digital CCD camera after acquiring a bright background and adjusting the histogram to the middle range. Quartz PCI imaging software was used for saving and uploading the images to the internet.

A light microscope (Vanox, model AHBS3) was used with either bright field (BF) or phase contrast illumination to examine semi-thick sections. Digital images were taken using camera (Sony, model DXC-950) and Northern Eclipse imaging software. Images were converted to black and white half tone, and the brightness and contrast was adjusted using Adobe Photoshop.

Chapter 3
Development of Fixation Methods for *M. nigrescens*

3.1 Introduction

Several different techniques for preparing the ocellus of invertebrates for TEM have been described (Siddiqui and Viglierchio, 1970; Burr and Webster, 1971; Burr and Burr, 1975; Burr et al., 2000a; and Insausti and Lazzari, 2000). Siddiqui and Viglierchio (1970) cut posterior to the ocellus of *Deontostoma californicum* in a cold fixative containing 5% glutaraldehyde in 0.1M phosphate buffer and post fixed in 1% OsO_4. However, Burr et al (2000a) used 3% glutaraldehyde in 0.5 M phosphate buffer to fix the ocellus of *M. nigrescens* and post-fixed in 2% OsO_4 for 3 hours. In another example, the ocellus of the insect *Triatoma infestans* was fixed in a mixture of 2.5% glutaraldehyde and 2.0% paraformaldehyde with sucrose and $CaCl_2$ for 3 hours before post fixing in 1% OsO_4 (Insausti and Lazzari 2000).

Although glutaraldehyde has been used extensively for TEM fixation, it has limited ability to stabilize lipid in the membranes and show contrasted structure. Also, it changes the appearance of structures due to artifacts or extraction during tissue fixation (Hayat, 2000). Post-fixing in OsO_4 results in better membrane preservation. However, osmication dissolves cytoskeletal proteins (Hayat, 2000). Using supplementary fixatives improves tissue preservation. Locke (1994) recommended uranyl acetate (UA) *en bloc* treatment after aldehyde fixation and without osmication. Chalfie and Thomson (1982) used

tannic acid to preserve the neuron microtubules of *Caenorhabditis elegans*.

One objective of this work was to develop a fixation protocol for improving the preservation of ultrastructure in *M. nigrescens*. In order to accomplish this, several fixation methods were tried. First, glutaraldehyde was combined with either paraformaldehyde or tannic acid, which act as supplementary fixatives. Also, UA *en bloc* staining was used after glutaraldehyde fixation, with or without osmium fixation. These results were compared by examining muscle spindles and nerve dendrites to reflect the effect of each fixative on protein and lipid preservations.

3.2 Experiments with fixation

The basic fixation protocol was described in Chapter 2. Experimental changes in the protocols and the results are summarized in Tables 1 and 2.

3.2.1 Addition of paraformaldehyde

Paraformaldehyde is used for tissue fixation because of its ability to penetrate the tissues rapidly. The Karnovsky fixative, which is a mixture of 2% paraformaldehyde and 2.5 % glutaraldehyde in 0.1 M sodium cacodylate buffer, was tried (Karnovsky, 1965).

The high osmolarity of the fixative caused the tissues to shrink. To prevent this, the fixative was applied to the tissue in steps of increasing concentrations at varied time intervals. Table 1 lists the concentration and time duration for each experiment. For preparations 7, 9B, and 9D

tissue shrinkage was avoided. However, when the graded concentrations were added more quickly (Table 1, Prep. 9A), tissue shrinkage occurred.

Figure 3.1 illustrates the effects of adding paraformaldehyde to glutaraldehyde fixative. Muscle myofilaments (A) and cytoskeleton of the amphidial dendrites (B) appear contrasted and well preserved. With this fixative, as well as other methods tried, the lipid membranes have a single rather than bi-layered appearance. With paraformaldehyde + glutaraldehyde, however, the cell membrane has a very low contrast and appears broken (B, insert). Thus, addition of paraformaldehyde improves protein fixation, but does not fix membrane lipid well.

In an attempt to improve lipid membrane preservation, post fixation in 2% OsO_4 was prolonged for an hour with additional microwave treatment (Table 1, Prep. 9B). However there was little improvement. When paraformaldehyde was used alone prior to glutaraldehyde (Table 1, Prep. 9D, Step 1, 2), neither lipid nor protein was preserved and extensive damage occurred (not shown). Thus, early preservation with glutaraldehyde is important.

3.2.3 Addition of Tannic Acid

To improve lipid membrane and protein fixation, tannic acid was added to the glutaraldehyde solution. A freshly prepared mixture of 1% tannic acid and 2.5% glutaraldehyde in 0.05 M cacodylate buffer was used before osmication (Table 2, Prep. 10D).

Muscle myofilaments are well preserved and a gray background indicates less extraction of cytoplasmic proteins (Fig. 3.4 C). However, membranes surrounding the muscle spindles and mitochondria are outlined with white halos, as is characteristic of tannic acid fixation.

Thus, the addition of tannic acid gives membranes an artifactual negative-stained appearance, although similar to paraformaldehyde, it improves protein fixation.

3.2.2 Use of uranyl acetate in place of or in addition to OsO_4

For comparing the effects of uranyl acetate *en bloc* treatment after conventional glutaraldehyde fixation, two experiments with different conditions were done. In Experiment 1, the specimen was fixed in 2.5% glutaraldehyde in 0.05 M Na cacodylate buffer and 1 mM $CaCl_2$ then treated with half saturated aqueous uranyl acetate over night at 60 °C (Table 2, Prep. 10B and 11B). In Experiment 2, the *en bloc* uranyl acetate treatment was done after conventional glutaraldehyde and OsO_4 fixation (Table 2, Prep. 10C and 11A).

Figures 3.2 and 3.3 compare *en bloc* staining in uranyl acetate with and without osmication. With both treatments the structures appeared well preserved and with sufficient contrast. However, best results were obtained with osmication. Without osmication, muscle myofilaments had a more uniform appearance against a gray background (Fig 3.2 A). With osmication, muscle myofilaments were more distinguishable (Fig 3.2 B). Mitochondria outer smooth and inner convoluted membranes are more contrasted after osmication (Fig. 3.2 B). Without osmication, mitochondria have an electron dense, poorly fixed appearance (Fig. 3.2 A).

With both treatments the microtubules and actin filament bundles in the nerve dendrites appear well preserved and contrasted (Fig. 3.3), however the latter are more densely clumped after osmication (B). Lipid membranes have fewer gaps after osmication (B, inset), thus appear to be

better preserved. Sections treated with UA *en bloc* staining could be examined without post-staining (Fig 3.4 B), but post-stained sections were sharper and more contrasted (Fig 3.4 A). Adding 1 mM $CaCl_2$ to the cacodylate buffer (Table 2, Prep 11A, 11B) produced better results by preventing tissue extraction, loss of cellular extents and stabilizing the cytoskeletal structure of the dendrite microtubules.

3.3 Conclusions

The results presented above indicated that supplements such as tannic acid, paraformaldehyde, and uranyl acetate had significant effects in improving the ultrastructure preservation of *M. nigrescens*. Addition of paraformaldehyde with the glutaraldehyde fixative resulted in well-preserved protein with lesser artifacts, yet membranes were poorly fixed. Increasing the fixation time with OsO_4, as well as pre-fixation with paraformaldehyde did not improve membrane fixation. Therefore, paraformaldehyde would not be recommended for conventional TEM fixation. Apparently, initial fixation with glutaraldehyde alone is important.

TEM observation showed that tannic acid improves protein preservation but results in halos around plasma membranes (Fig. 3.4 C). Chalfie and Thomson (1982) reported an improvement in protofilament preservation with tannic acid fixation. However, the artifactual effect of tannic acid on plasma membranes was similar in *C. elegans* (Fig. 3 in Chalfie and Thomson, 1982).

These results confirm Locke's finding that glutaraldehyde/UA treatment gives high contrast and well-preserved tissue similar to the conventional osmication procedure (Locke, 1994). Thus UA acts as a

good fixative for lipid, proteins and myofilaments. The difference in contrast between muscle myofilaments fixed in osmium and without osmium (Fig. 3.2) could be a result of the OsO_4 extracting some cytoplasmic proteins. Also, the difference in appearance of mitochondria with and without osmication (Fig. 3.2) suggests that glutaraldehyde alone does not fix mitochondrial membranes well enough leaving the membranes impermeable to small solutes such as UA and resulting in mitochondria with a poorly fixed appearance (Fig. 3.2 A).

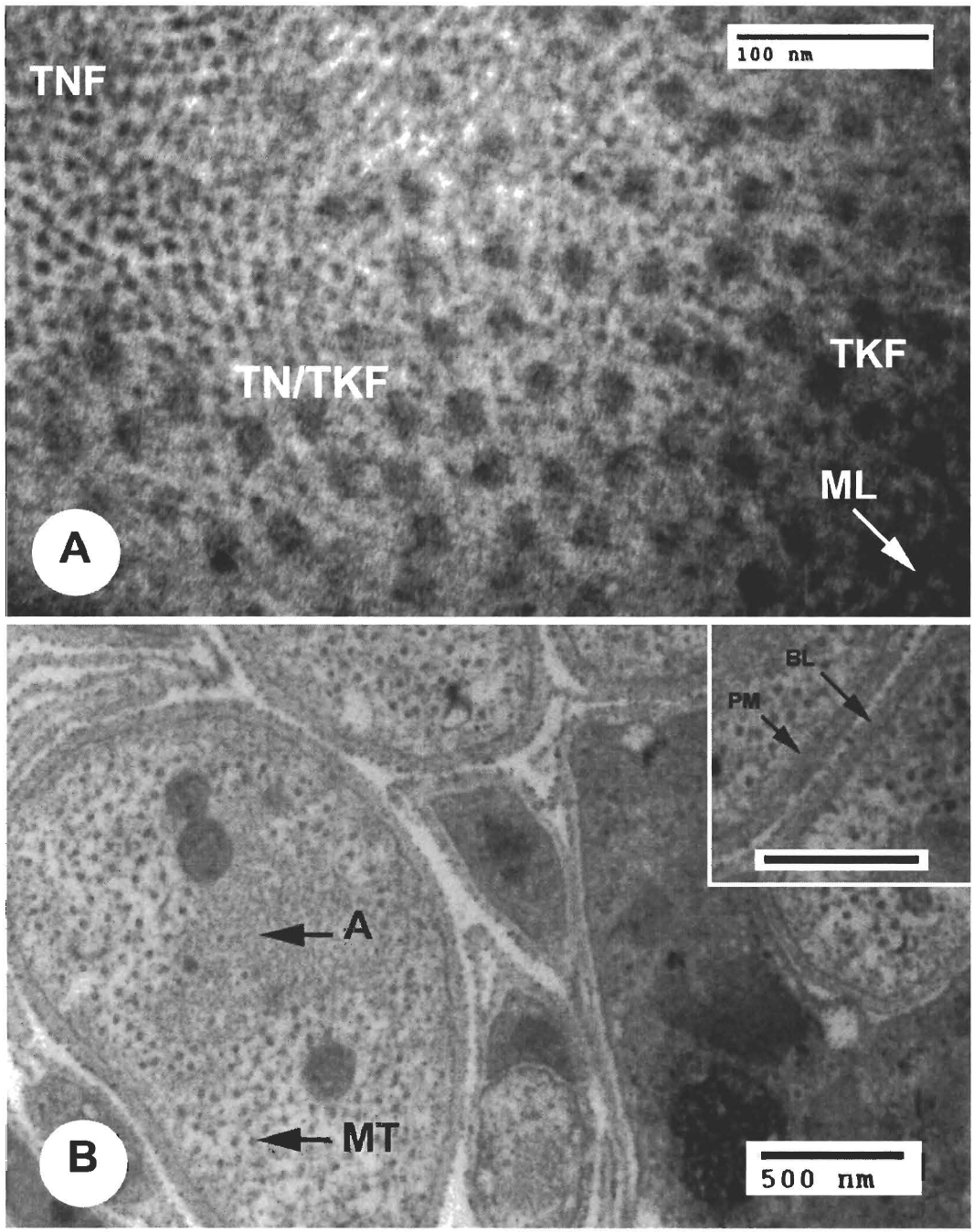

Figure 3. 1. Effects of introducing paraformaldehyde (Prep. 7). (A) Muscle filaments showing the well preservation of proteins. (B) Nerve dendrites showing good fixation of cytoskeletal filaments. Inset, showing poor fixation of plasma membrane. *Bar.* 500 nm.

A, actin filament bundle; MT, microtubule; BL, basal lamina; PM, plasma membrane; TKF, region of thick filaments; TNF, region of thin filaments; TN/TKF, region of thin and thick filaments; ML, M-line.

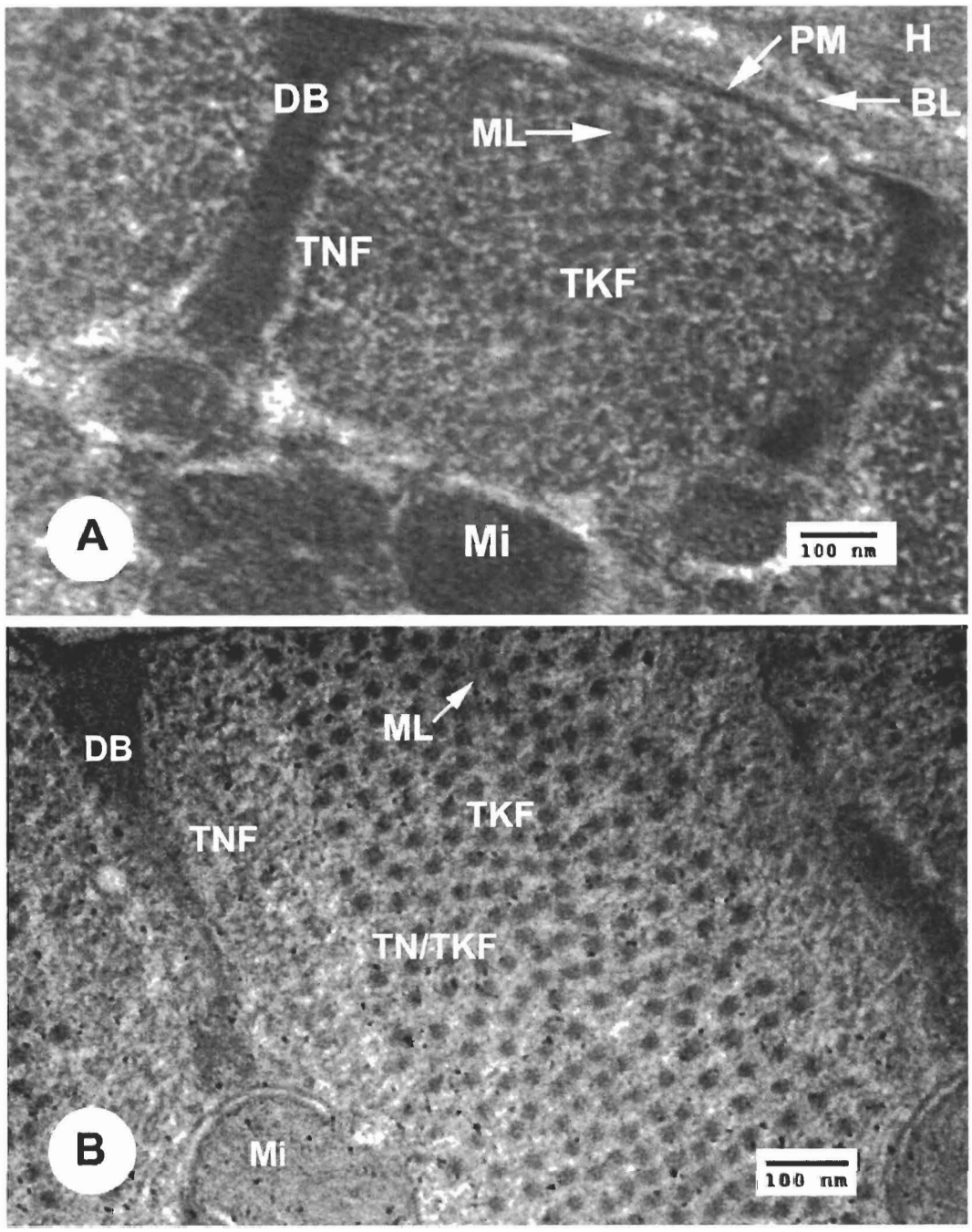

Figure 3. 2. Effects of uranyl acetate *en bloc* staining on the appearance of the muscle. (A) After only glutaraldehyde fixation (Prep. 11B). (B) After glutaraldehyde and OsO_4 fixation (Prep. 11A).

BL, basal lamina; DB, dense body; H, hypodermis; TNF, region of thin filaments; TKF, region of thick filaments; TN/TKFML, region of thin and thick filaments; ML, M-line; Mi, mitochondria; PL, plasma membrane.

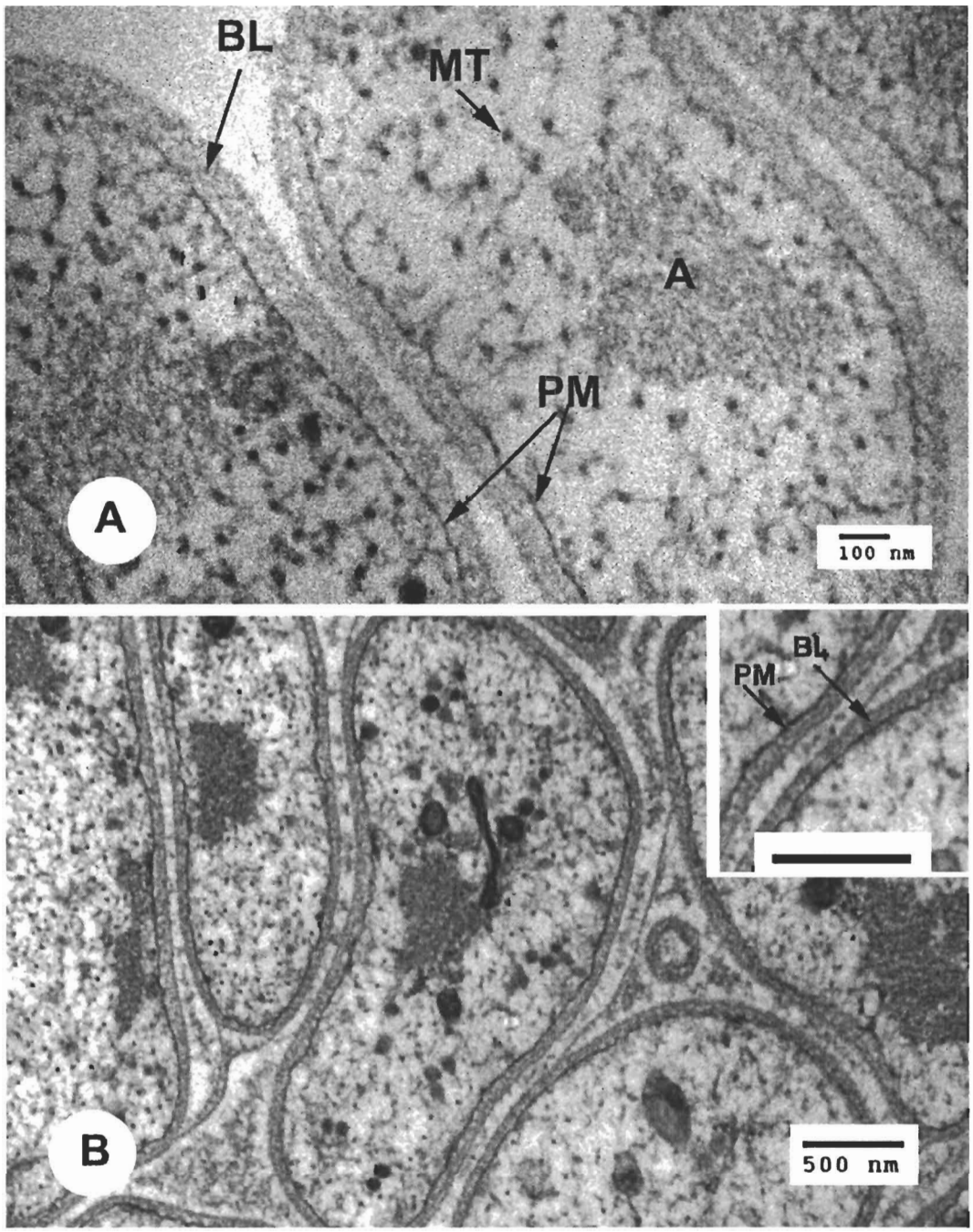

Figure 3. 3. Effects of uranyl acetate *en bloc* staining on the appearance of the amphidial dendrites. (A) Without OsO_4 post-fixation (Prep. 11B). (B) With OsO_4 (Prep. 11A). Inset, showing well fixation of membrane. *Bar*. 500 nm.

BL, basal lamina; PL, plasma membrane; A, region of actin filaments; MT, microtubule.

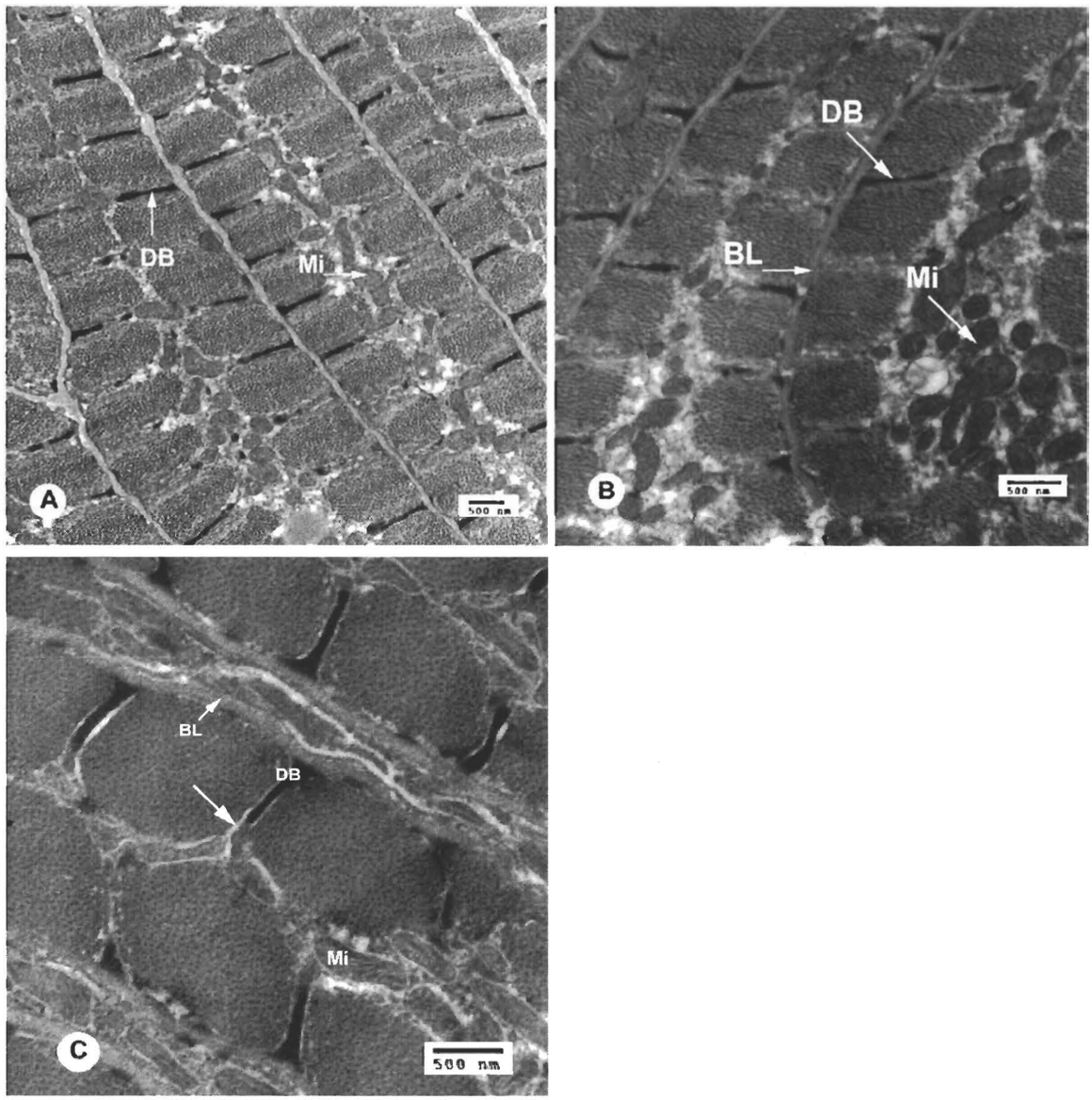

Figures 3. 4. Effects of various fixation and staining protocols on appearance of muscle.

A, B. Glutaraldehyde/osmium fixations and uranyl acetate *en bloc* staining (Prep. 11A). (A) After post-staining sections with uranyl acetate and lead citrate. (B) Without post- staining sections.

C. Tannic-acid fixation (Prep. 10D). Arrow, negative-stained appearance of membrane.

BD, dense body; BL, basal lamina; Mi, mitochondria.

Table 1. Experiments with paraformaldehyde and OsO4

Variables	Prep. 7	Prep. 9A	Prep. 9B	Prep. 9D	
Aldehyde Fixation					
				Step (1)	**Step (2)**
Types	Glut./Paraform.	Glut./Paraform.	Glut./ Paraform.	Paraform.	Glut./Paraform.
Conc.	2.5%, 2%	2.5%, 2%	2.5%, 2%	**0.3%**	2.5%, 2%
Buffer	Na caco.	Na caco.	Na caco.	Na caco.	Na caco.
Final conc.	0.1 M	0.1 M	0.1 M	0.05M	0.1 M
Step concs.	1:10, 1:5, 1:2	1:10, 1:5, 1:2, 1	1:10, 1:5, 1:2, 1	100%	1:10, 1:5, 1:2, 1
Step time (min.)	15, 10, 20, Mw, 60	**5, 5, 5**, Mw, o.n	5, 10, 20, Mw, o.n	20	5, 10, 20, Mw, 60
Post Fixation					
OsO_4	2%	2%	2%		2%
Buffer	Water	Water	Water		Water
Time (min.)	Mw	Mw	Mw+**60**		Mw
Results	Well preserved protein. Poor membrane fixation Fig. 3.1	Tissue shrinkage	Poor membrane fixation as in Prep. 7		Poor membrane fixation. Low contrast.

Mw, microwave treatment; o.n., over night; min., minute

Table 2. Experiments with uranyl acetate and tannic acid

Variables	Prep. 10B and Prep 11B	Prep. 10C and Prep. 11A	Prep. 10D
Aldehyde Fixation			
Types	Glut.	Glut.	**Glut.+Tannic acid**
Conc.	2.5%	2.5%	2.5%, 1%
Buffer	Na caco. (Prep. 10B) Na caco./**$CaCl_2$** (Prep. 11B)	Na caco./**$CaCl_2$**	Na caco.
Conc.	0.05 M/1mM	0.05 M/1mM	0.05 M
Time (min.)	Mw, 60	Mw, 60	Mw, 60
Post Fixation			
OsO4	**None**	2%	2%
Buffer type		Water	Water
Time (min.)		Mw+10	Mw+10
Uranyl Ac. *en bloc*			
Conc.	**0.5 Saturated**	**0.5 Saturated**	—
Time (min.)	o.n at 60 °C	o.n at 60 °C	
Section Stain	**None** or 10m UA, 5m LC	**None** or10m UA, 5m LC	12m UA, 6m LC
Results	Well preserved muscle and contrasted membrane. Fig. 3. 2 A, 3. 3 B	**Best fixation** of both membrane and muscle. Fig. 3. 2 B, 3. 3 B, 3. 4 A, B.	Well preserved muscle. Membrane with negative appearance Fig. 3. 4 C

UA, uranyl acetate; LC, lead citrate; o.n., over night; Mw; microwave treatment.

Chapter 4
Mermis nigrescens Photoreceptors

4.1 Introduction

This work has two main objectives: first, to locate the photoreceptor in the adult female's ocellus, and second, to compare it to the other sensory structures in the anterior head.

During the early stages of this research, I tried to use the fluorescent label DiI (fluorescein isothiocyanate, 1, 1-dilinoleyl-3, 3, 3′, 3′-tetra-methylindocarbocyanine perchlorate) to identify the sensory neurons. DiI diffuses in the cell membrane, resulting in fluorescent labeled membrane. I experimented with two different techniques to apply DiI. The dye filling technique, applying DiI to the whole worm as described in (Hedgecock, et al., 1985), failed because DiI stained other lipid membranes of the internal structures, and making the photoreceptor membrane indistinguishable from the other structures. The intracellular injection technique, in which DiI is applied to the cell bodies in the brain region and then taken up by the dendritic processes (Godement et al, 1987), also failed. This was due to the small size of the nematode, which made the injection process very difficult. Also, the encircling cylinder of dense pigment made observation of the central nerve tracks difficult.

Therefore, I investigated the use of transverse serial sectioning of the ocellus of the worm and examining the results with both light and transmission electron microscopy (TEM). Analyzing the ultra-structural morphology has provided insights as to the function of the nervous

system of a wide variety of nematode species (Ward et al., 1975; Burr and Burr, 1975; Coomans, 1981; Burr, 1984; Strote, 1996; Li et al., 2000). This technique proved successful with *M. nigrescens* because it allowed me to distinguish a possible photoreceptor structure in the ocellus.

4.2 Methods

4.2.1 Serial sectioning of ocellus

Five anterior tips of *Mermis* nematodes: two of adult females, one of an immature adult female, and two of juveniles, were initially fixed using preparations 7, 11A, and 11B (as described in chapter 3). Then, they were cut into serial transverse sections. Ultra-thin sections, approximately 60 nm thick, were placed in order, while semi-thick transverse sections, approximately 0.5 μm thick, were collected and placed on numbered glass slides accordingly. To determine the approximate location of the photoreceptors, serial sectioning was started from the anterior tip to the end of the pigmented region. Approximate distances were calculated by multiplying the numbers of ultra-thin and semi-thick sections by their respective thickness.

4.2.2 Montage for sections

The process of montaging TEMs of a transverse section through *Mermis* ocellus was accomplished in two stages. The first stage involved acquiring digital images that covered the transverse section, as described in Chapter 2. The second stage involved integrating these images into a single image showing the whole transverse section.

The digital images were photographed with a magnification of 7000 X. The top left corner of a section was first positioned under the camera

to capture an image. Then, in order to create overlapping photographs, the section was moved horizontally in constant increments of ΔX each, where ΔX is approximately two thirds of the image width. After completing a horizontal strip, the section was moved vertically by a distance ΔY, which is approximately two thirds of the image height, to capture another horizontal strip, and so on.

The integration of digital images was accomplished using the software program Adobe Photoshop version 6. All the acquired images were positioned to reflect the actual location within the section and construct a single image of a transverse section.

4.3 Anterior morphology

Figure 4. 1 illustrates the general anterior morphology of the adult female. Table 3 summarizes the approximate measurements through the anterior head in the adult female.

Table 3: Measurements through the head of mature adult female

Structure	Level A	Level B	Level C	Level D	Level E	Level F
Total diameter	125 µm	137.5µm	150 µm	157 µm	180 µm	190 µm
Cuticle thickness	21 µm	18µm	28 µm	28 µm	22 µm	22 µm
Outer diam. of pigmentation	0	0	106 µm	94 µm	94 µm	100 µm
Inner diam. of pigmentation	0	0	62 µm	43 µm	34 µm	31 µm
Muscle thickness	0	0	0	5.5 µm	20 µm	20 µm

M. nigrescens is covered with a thick cuticle, approximately 21.5 μm thick, compared to other Mermithid nematodes, where the average thickness is about 4.5 μm (Batson, 1979). The cuticle consists of three layers: the homogeneous outermost layer, the spongy median zone, and the fibrous basal layer (Gans and Burr, 1994). At the tip of the head, the cuticle surface has the smooth appearance that is typical of most Mermithid nematodes (Techesunov and Hope, 1997). A thickening of the cuticle about 90 μm from the tip called the collar region distinguishes the adult and immature females from the juvenile (Figs. 4.1) (Table 3, Level C and D).

Underneath the cuticle, a single layer of longitudinal muscle cells appears at about 110 μm from the tip with a thickness that gradually increases from about 5 μm to about 20 μm (Fig. 4.2 D-F; Table 3). The muscle spindles consist of longitudinal columns of sarcomeres with adjacent columns staggered to form the unusual pattern in cross sections typical of obliquely striated muscle (Fig. 3.4 A, B). Within each sarcomere, thin filaments are attached to the dense bodies and thick filaments are connected to each other by the M-line (Fig. 3.2).

A thin layer of hypodermis, about 2.4 μm thick, lies between the muscle and the cuticle, and among other functions, is responsible for forming the cuticle. The inner surface of the hypodermis contains numerous lamellae that could have an active transport system. This system allows the entry of nutrients required for growth, especially during the parasitic stage (Poinar and Hess, 1977). Half desmosomes and intermediate filaments connect the basal lamina across the hypodermal cytoplasm to the cuticle (Fig 3.2, 3.4). The dense bodies, basal lamina, and hypodermis connect the muscle sarcomeres directly to the cuticle. It

is suggested that this transmits the force of the muscle contraction radially to the cuticle rather than along the sarcomere columns to their ends (Burr and Gans, 1997). The longitudinal muscles of Mermithids have a unique arrangement into two sub-dorsal and four sub-ventral bands divided by medial expansions of the hypodermal cells (Fig. 4.2 E, F). The non-muscular pharynx is another characteristic of Mermithids.

The cell bodies of the anterior sensory nerves are located behind the cephalic ganglion, about 500 μm from the tip, and project dendrites anteriorly. The dendrites are segregated into tracks that run alongside the non-muscular pharynx to the sensilla in the anterior tip (Fig. 4.1). There are two lateral amphidial tracks, and two sub-dorsal and two sub-ventral cephalic tracks (Fig. 4.4).

The cephalic track has a smaller diameter (about 6 μm) than the amphidial track (16 μm). Also, the number of the cephalic dendrites (5 to 7) is less than the number of amphidial dendrites (19 to 21) (Fig. 4.3 B, 4.4). Anteriorly, the cephalic and amphidial tracks innervate sensilla. Figure 4.2 B of a transverse section at level B (Fig. 4.1) shows the arrangement of the sensilla. Typically, each sensillum consists of a variable number of neurons that penetrate into the sheath cell.

Figure 4.2 A shows two of the four cephalic channels about 5μm from the tip. Each cephalic sensillum contains four dendritic processes (Fig. 4.3 A). In *M. nigrescens*, the cephalic processes lack a basal body and contain numerous microtubules (Lee, 1974) and thus the material inside the processes in Fig. 4.3 A (arrow) may be microtubules sectioned obliquely. These modified cilia invaginate into a sheath cell. The sheath cell apparently has vesicles or microvilli enclosing an electron-dense material (Fig. 4.3 A). The DiI filling technique showed that the cephalic

sensilla open to outer environment through a pore at the anterior tip (not shown).

The amphidial sensilla are located about 60 μm posterior to the tip with a length of about 20 μm and open to the outer environment laterally. A transverse section, between level A and B (Fig. 4.1), showed that the amphidial channel, containing modified cilia, is enclosed by a sheath cell that has numerous infoldings that may have a secretory function as in *Gastromermis boophthorae* (Batson, 1978).

In *Mermis,* approximately 55 - 70 μm from the tip, there are inner and outer labial sensilla that may have an arrangement of 3 + 3, as in another Mermithid nematode, *Gastromermis boophthorae* (Batson, 1978). A TEM showed that the sheath cell of the inner labial sensilla encloses two dendritic processes (Fig. 4.3 D). The structure resembles that of modified cilia of inner labial processes of other nematodes (Endo, 1980; Albert and Riddle, 1983). In *C. elegans*, the inner labial sensilla are characterized by two cilia that contain microtubules and electron-dense core (Albert and Riddle, 1983).

The sheath cell of the outer labial sensillum encloses a dendritic process (Fig. 4.3 C). Mechanoreceptor processes of nematodes usually contain microtubules embedded in electron-dense materials (Ward et al., 1975; Strote et al., 1996). In both the inner and outer labial channels, the dendritic processes penetrate into a sheath cell that has numerous lamellae enclosing a cytoplasm (Fig. 4.3 C, D). A similar microvillar structure was seen in *Onchocerca volvulus* (Strote et al., 1996).

4.4 Morphology of the ocellus and location of the photoreceptors

4.4.1 Morphology of the pigmented structure

The ocellus of *M. nigrescens* is unique in location and morphology. The single cylindrical bright-red shadowing structure extends from approximately 80 μm posterior to the tip to a length of about 250-300 μm with a diameter of 106 μm and an approximate outside diameter of 100 μm (Table 3; Fig. 4.1). This is formed by projections of hypodermal cord cells into the pseudocoelom (Figs. 4.2 C-F). Note that the cytoplasm of the hypodermal cells is densely filled with electron dense inclusions about 0.3-1.0 μm in diameter (Figs 4.4, 4.7, 4.9, 4.11). These are visibly red colored in light micrographs (Figs. 4.2 C-F) and have been shown to be hemoglobin crystals by their dichroic spectrum (Burr and Harosi, 1985). The crystals displace the nuclei toward the periphery (Fig. 4.4, inset), unlike in the typical hypodermal cell morphology seen in J4 juveniles and immature females (see Chapter 5). Extensions of the hypodermal cells form a cylindrical shape that encircles the pharynx and the central sensory tracks (Figs 4.2 C-E, 4.4, 4.7, 4.9). However, posterior to the pigmented region, a thin layer of the pseudocoelom divides the hypodermal cells (Fig. 4. 2 F). The hypodermal cells at level E and F form of six bulges: one dorsal, one ventral, two laterals, and two sub-ventral (Fig 4.2 E, F).

4.4.2 Photoreceptor location

The putative photoreceptor location will be described at two levels, first: level C to D, and second: level D to E (Fig. 4.1).

In TEMs at level C to D, the collar region, lamellae are observed to project from one of the nineteen amphidial dendrites in each track (Figs.4.4 - 4.8). These could be the photoreceptors that were predicted from behavioral observations (Burr and Babinszki, 1990). The lamellae invaginate a supporting cell with an electron-dense cytoplasm, which is probably a sheath cell (Fig. 4.6). The other amphidial dendrites, which lack lamellae and are enveloped by a basal lamina (Fig. 4.6 A), pass anteriorly to the amphid where they become enclosed by a sheath cell in the amphidial sensilla as usual for chemosensory dendrites. The lamellar projections in this region are more than 10 μm long and about 330 nm thick. Another adult female was examined to verify this observation. A similar structure exists in the same collar region, about 85 μm posterior to the tip.

In TEMs at level D to E, where the body wall muscle begins to appear, the multilamellar dendritic processes are located more ventrolaterally, while the lamella have significantly decreased in size (Fig. 4.7, 4.8). At level E, the lamellae have disappeared and it is difficult to distinguish the putative photoreceptor dendrites from the other amphidial dendrites (Fig. 4.9, 4.10). At this level, the sheath cell nearly fills the amphidial track (Fig. 4.9).

The sheath cell is analogous to the glial gland of insect's ocellus (Isausti and Lazzari, 2002). Its cytoplasm is distinguishably denser than the cytoplasm of the lamellae and the dendrites. A number of dense bodies are located in the cytoplasm. An increase of the size of the sheath cell was noticed in more posterior sections (Fig. 4.9).

At level C, an unusual muscle type appears free in the pseudocoelom (Fig. 4.3 A, 4.4). Eight oval-shaped muscle fibers are

located adjacent to the cephalic nerve tracks. Each fiber consists of a spindle that is similar to the spindle of body wall muscle. Their function is unknown.

4.5 Discussion

4.5.1 Can the lamellar structure be the photoreceptor?

Most nematode sensory organelles are associated with a sheath cell. Therefore, the fact that the lamellae penetrate into a sheath cell (Fig. 4.6) supports a possible sensory function. Since the lamellae are located in the amphidial track at a large distance posterior to the anterior sensilla, they appear not to have an ordinary chemosensory sensory function.

The photoreceptor organelles in nematodes have either multiciliary (e.g. *Oncholaimus vesicarius)* (Burr and Burr, 1975) or multilamellar structures (e.g. *Deontostoma californicum, Chromadorina bioculata, Enoplus communis*, *Diplolaimella* sp) (Siddiqui and Viglierchio, 1970a,b; Croll et al., 1975; Van De Velde and Coomans, 1988). In other animals, a multimicrovillar structure is also observed. These structures serve to increase the surface area of the cell and thus increase sensitivity by increasing the number of rhodopsin molecules available to capture a photon. The similarity of the multilamellar dendritic processes described here in the *Mermis* ocellus to known photoreceptor organelles supports the possibility that they could be photoreceptive organelles.

In female *M. nigrescens,* TEMs through the anterior tip showed modified cilia of the inner labial receptors, outer labial receptors, and cephalic receptors (Fig. 4.3). However, it is unlikely that these modified

cilia have photoreceptor function. The cilia either open to the outer environment through pores or are embedded within the cuticle, thus, they are more likely chemoreceptive or mechanoreceptive (Ward, 1975; Wright, 1980). Lamellar projections of a sheath cell are observed surrounding the inner and outer labial receptors in *Mermis* (Fig.4.3) as well as other nematodes. However these have a secretary function as shown by Endo (1980). A sheath cell cannot have a photosensory function because it is a non-neural cell and doesn't give synapses to any other cell (Ward, 1975).

To be useful in phototaxis, a photoreceptor organelle needs to be capable of being shaded by a pigment. The pigment casts a shadow on adjacent photoreceptors to provide the eye with directional sensitivity towards light. In *M. nigrescens,* experimental manipulation of the behavior proved that the photoreceptors must be located within the cylindrical shadowing structure (Burr and Babinszki, 1990). The multilamella dendritic processes described in this study are the only sensory structures that are similar to photoreceptor organelles in the anterior and are located inside the pigmented cylinder. Therefore I conclude that the lamellar projections from two amphidial dendrites are probably the predicted photoreceptor organelles.

Analogous morphology is found in the wing and the finger structures of the amphidial neurons (AWA, AWB, AWC and AFD) that were described in *C. elegans,* a nematode that has photosensitive behavior but no ocellus (Burr, 1985). The finger and wing neurons are possible candidates for photoreceptors as their modified cilia have a large membrane area and penetrate the sheath cell of the amphidial sensilla. However, they have been shown to be thermosensitive or chemoreceptive

(Bargmann. 1993). Their possible role in the light response in *C. elegans* is still unclear and needs further study. This can be achieved by laser-ablation experiments that become possible after 3D reconstruction of the L1 nervous system in order to provide a map of the cell body locations (Ward et al., 1975; Li et al., 2000a; Li et al., 2000b).

4.5.2 Implications for evolution of photoreceptors in *M. nigrescens* and other nematodes

The multiciliary photoreceptors in *O. vesicarius* are located within the amphidial sensilla. The aberrant cilia, a group of 10 modified cilia, are similar to the chemoreceptor cilia in entering the amphidial duct and aperture; however; they project medially to a position where they can be shadowed by the eyespot pigment (Burr and Burr, 1975). Therefore, these photoreceptive cilia might have evolved for photoreception from one of the amphidial chemoreceptor cilia (Burr and Burr, 1975; Burr, 1984).

It is possible that the potential photoreceptor described here for *Mermis* may also have evolved from an amphidial chemoreceptor. One of the dendrites in the amphidial track forms multilamellar membranes that project perpendicular to the body axis of the nematode. In addition, the lamellar dendrite ends anteriorly where the ocellus starts rather than continuing to the amphidial sensillum where the other dendrites have a chemosensory function.

Burr (1984) hypothesized that nematode photoreceptors belong to a different line in evolution that includes the epigenous type of photoreceptors. The presence of multilamellar membranes at the apical end of a dendrite suggests that *Mermis* could belong to the epigenous type.

In *D. californicum*, the multilamellar photoreceptors in the cup-shaped pigment structure originate from one of the cephalic dendrites (Siddiqui and Viglierchio, 1970a,b). Thus it is possible that in this species, the multilamellar photoreceptor organelles, unlike in *Mermis*, may have evolved from a cephalic chemoreceptor.

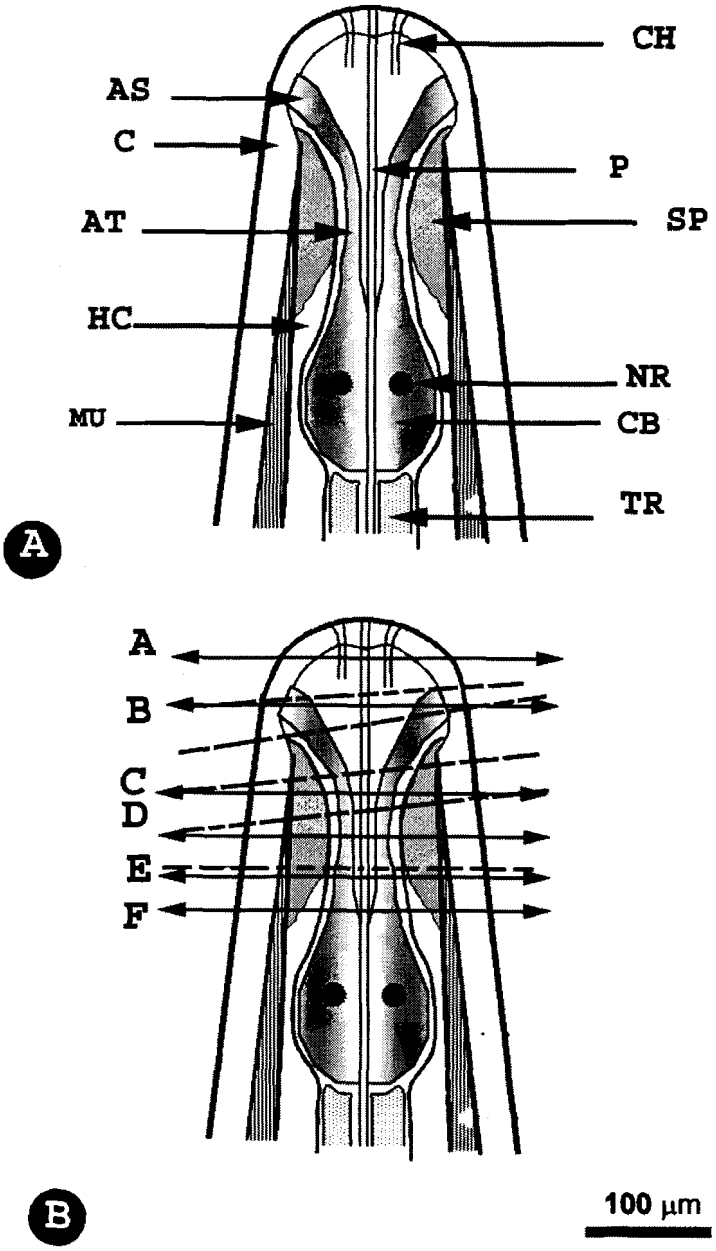

Figure 4. 1. Anterior tip of a mature adult female of *Mermis nigrescens*. Longitudinal section through the midline showing dorsal view (A) Illustrating the shadowing pigment location and the anterior morphology. (B) Illustrating the location of transverse sections to be illustrated in subsequent figures. Solid lines, sections through a mature female. Broken lines, sections through an immature female. C, cuticle; MU, muscle; HC, hypodermal cells; SP, shadowing pigment; TR, trophosome; NR, nerve ring; AT, amphidial track; AS, amphidial sensillum; CB, cell bodies; P, pharynx; CH, cephalic channel.

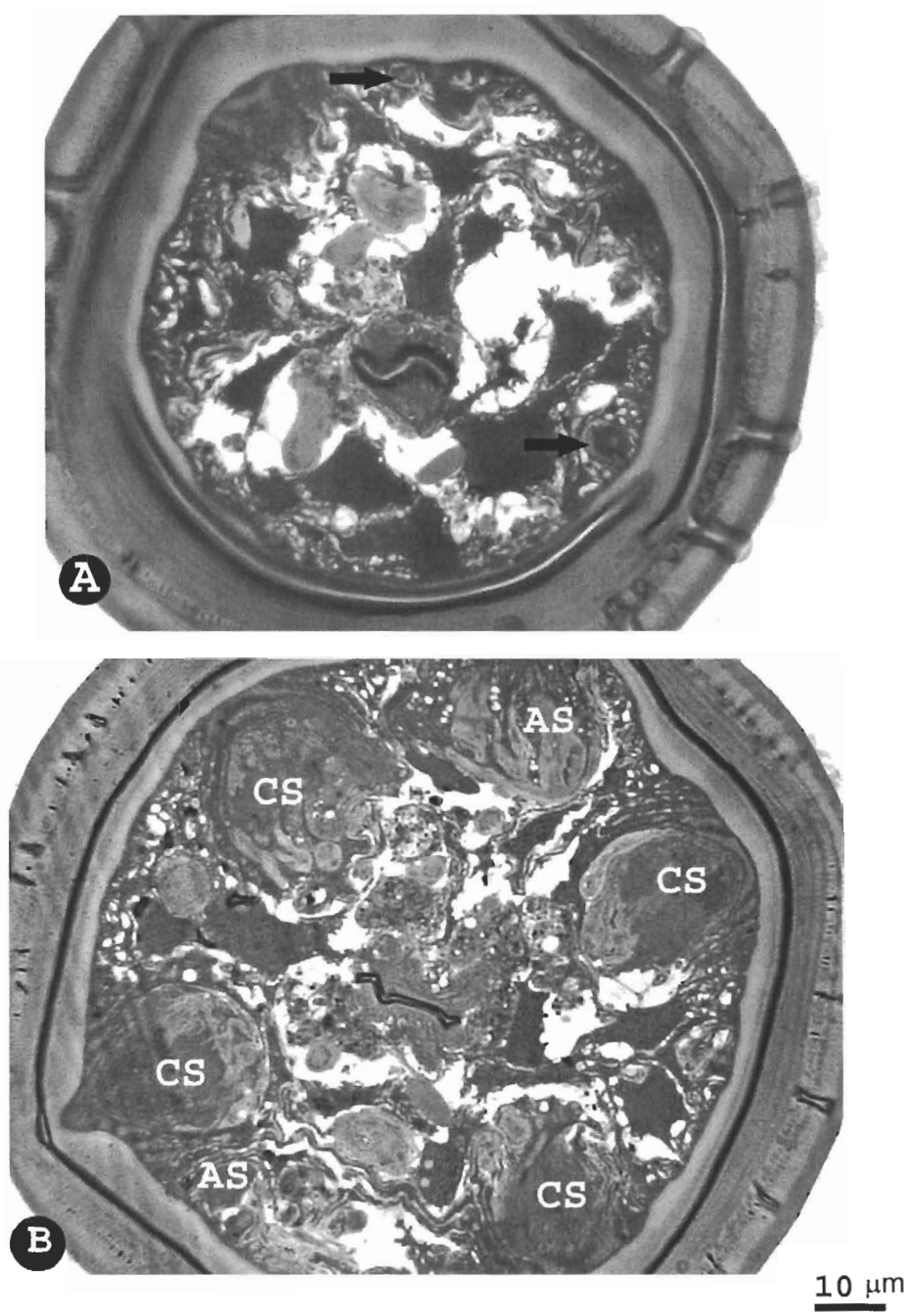

Figure 4.2. Morphology of a mature adult female. Light micrographs of transverse semi-thick sections at different levels through the anterior:

A, B. Sections through the different levels of sensilla. (A) Near the tip at level A (Fig. 4.1), two of the four cephalic channels (Arrows) located near the cuticle. (B) At level B (Fig. 4.1) that passes through the four cephalic sensilla (CS). The two lateral amphidial sensilla (AS) are sectioned at different levels.

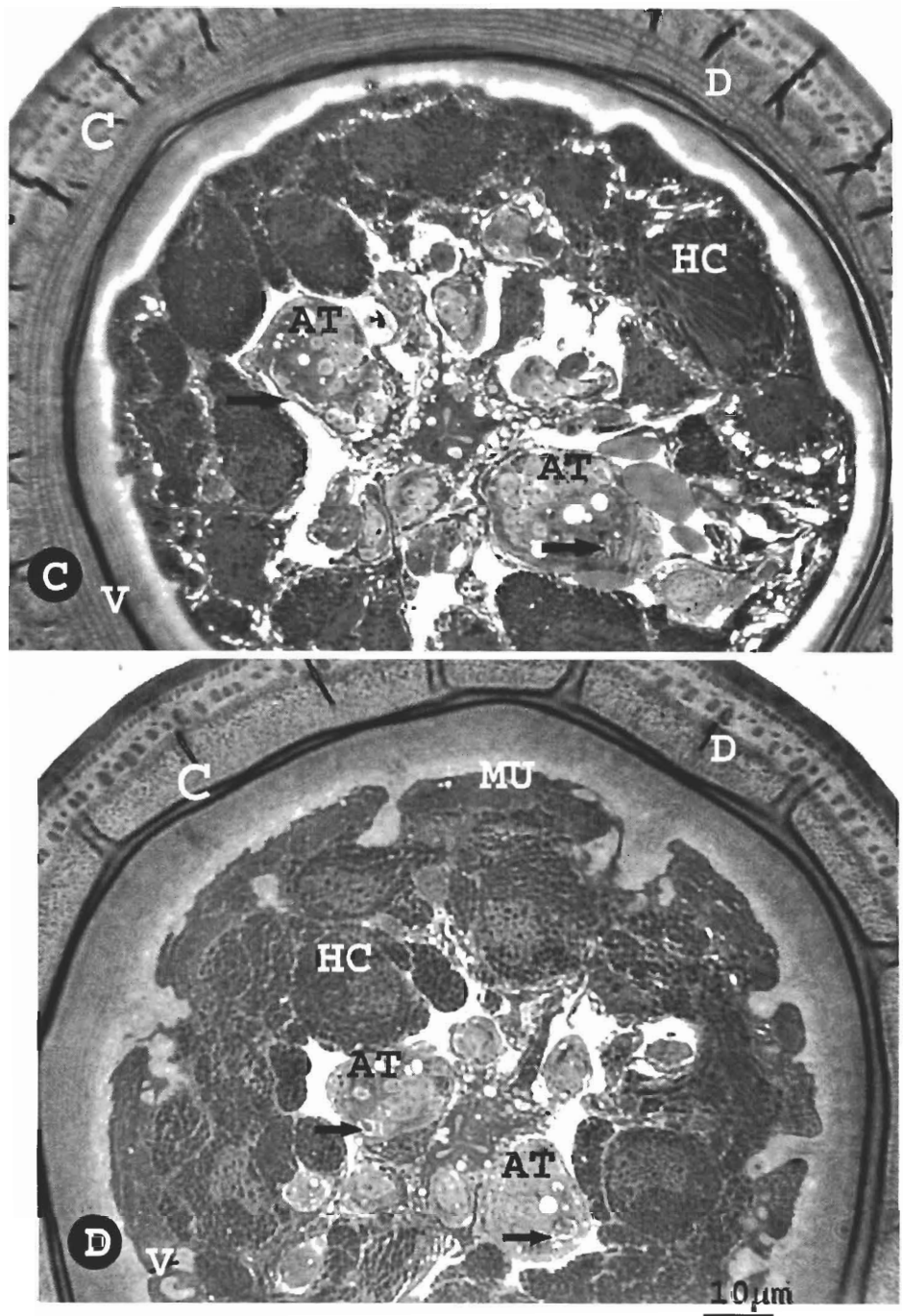

C, D. Transverse sections at the level of the collar and the beginning of the cylindrical ocellus (A) (Fig. 4. 1, level C) illustrating the location of the multilamellar process, a possible photoreceptor (arrows) (D) Section through the ocellus at the level of the lamellar photoreceptor structure (arrows) (Fig. 4. 1, level D) showing the pigmented hypodermal cells surrounding the pseudocoelom and nerve tracts. The muscle cells (MU) have just appeared. D, dorsal side; V, ventral side; C, cuticle; HC, hypodermal cells, AT, amphidial track.

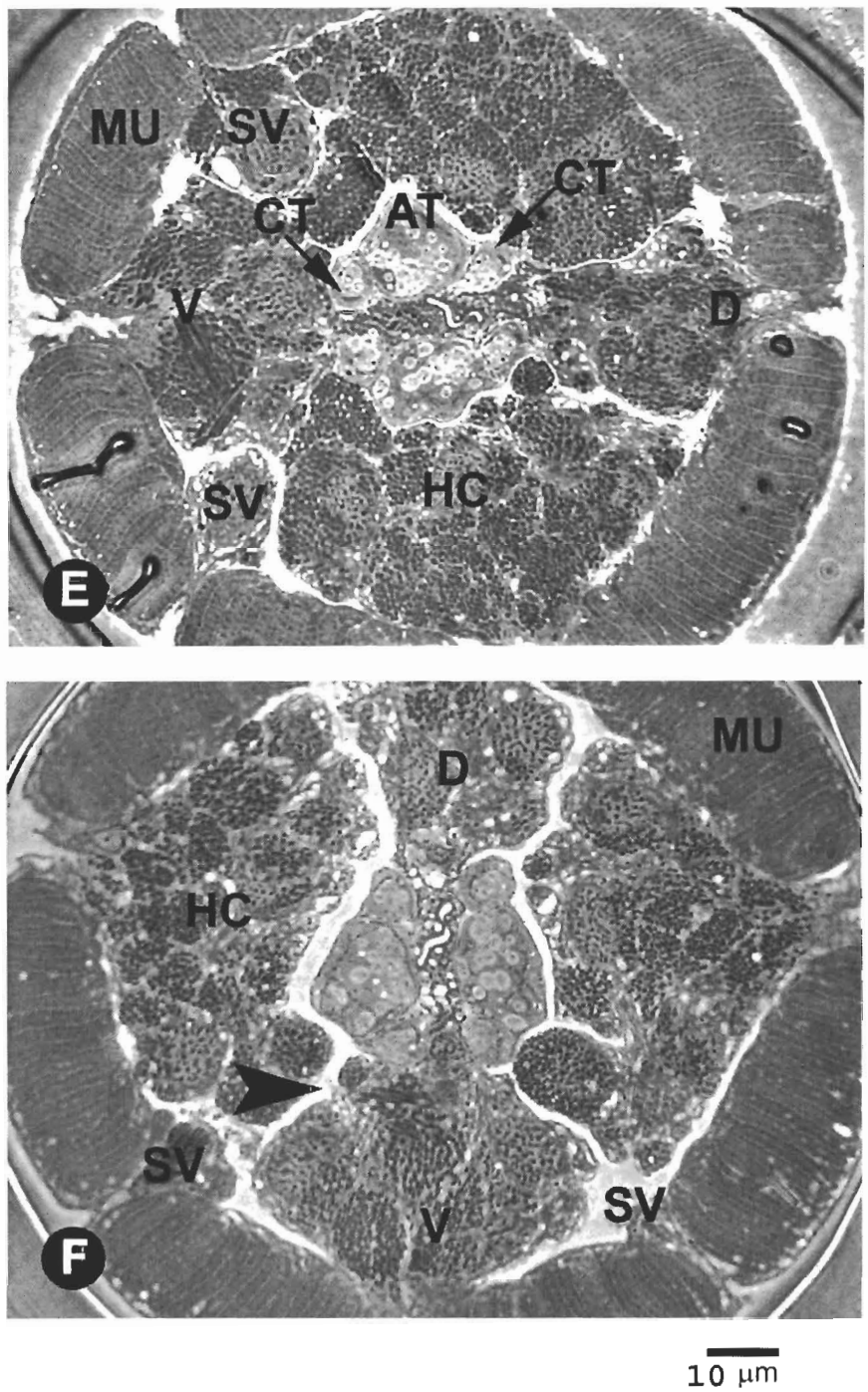

E, F. Posterior transverse sections where the pigmented hypodermal cells separate the developed muscle spindles into six bands. (E) The ocellus at level E (Fig. 4. 1). Note the movement of the cephalic tracks (CT) to dorsal and ventral positions adjacent to the amphidial tracks (AT). (F) The most posterior region of the ocellus (Fig. 4. 1, level F). The six projections of the hypodermis divided by a thin layer of pseudocoelom (Arrow head). D, dorsal side; V, ventral side; HC, hypodermal cell; SV, sub-ventral hypodermal cord; MU, muscle.

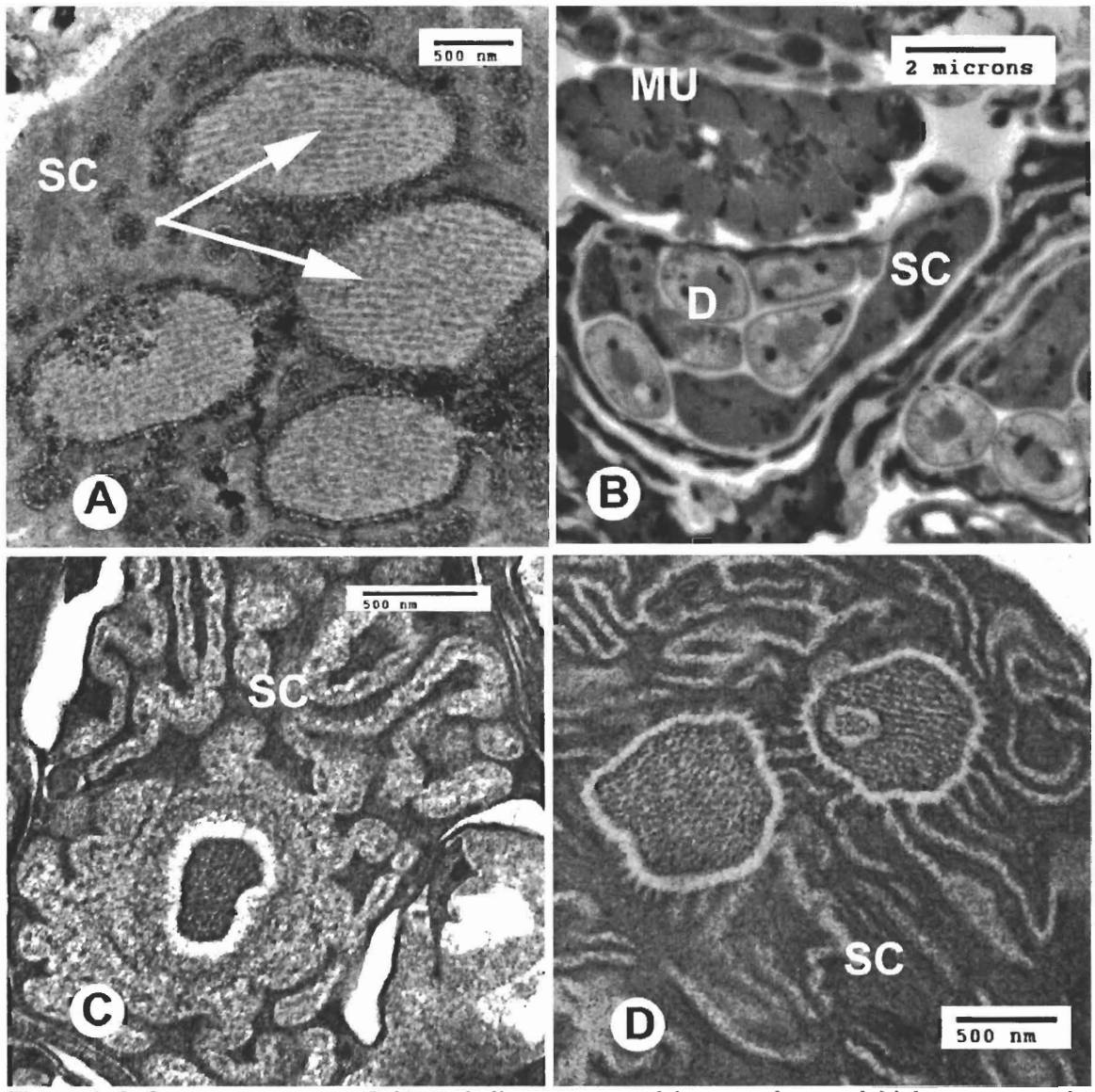

Figure 4. 3. Sensory structure of the cephalic neurons and inner and outer labial neurons at the anterior of the mature female (Fig. 4. 1, level B). (A) Cephalic sensillum. (B) Cephalic track (Fig. 4. 1, level C). (C) Outer labial sensillum. (D) Inner labial sensillum. SC, sheath cell; D; dendrite; MU, muscle.

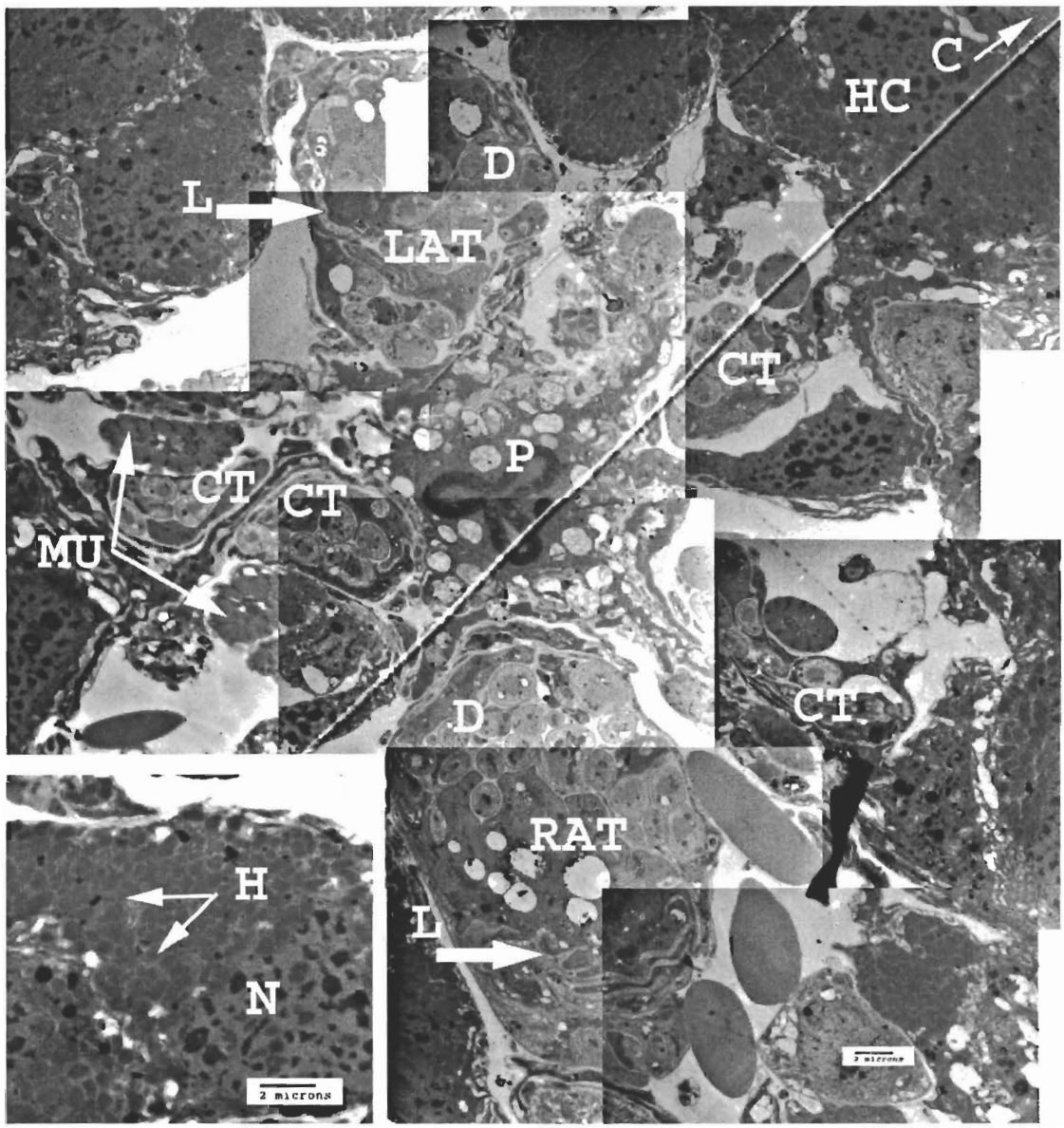

Figure 4. 4. Montaged TEMs of a transverse section at the collar region (Fig. 4. 1, level C). Inset: Higher magnification of hypodermal cytoplasm. Fully developed lamellar structures (L) (Arrows) in the left (LAT) and right (RAT) amphidial tracks. The hypodermal cells (HC) that consist of a peripheral nucleus (N) and cytoplasm packed with numerous densely-packed hemoglobin crystals (H) surround the central region containing nerve tracks. CT, cephalic track; MU, muscle band; P, pharynx; C, cuticle; D, dendrite.

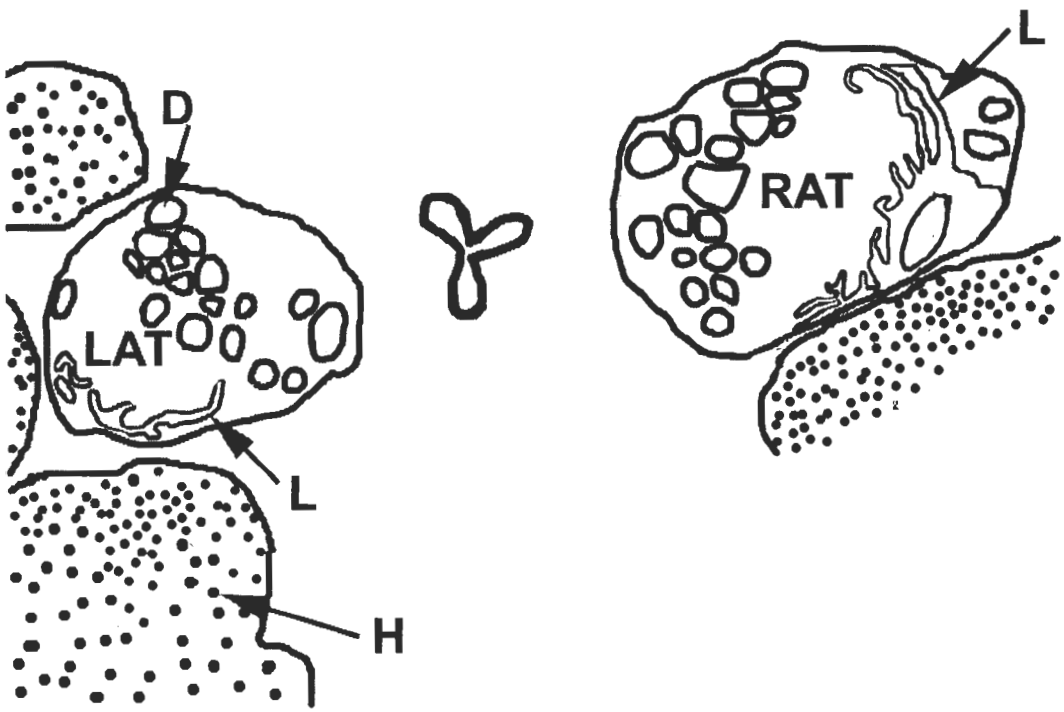

Figure 4. 5. Outlines of structures in Fig. 4. 4 illustrating a dendrite in each amphidial track, left (LAT) and right (RAT) track, projecting lamellae (L), a possible photoreceptor structure. The tracks are surrounded with hypodermal cells containing hemoglobin crystals (H). D, dendrite.

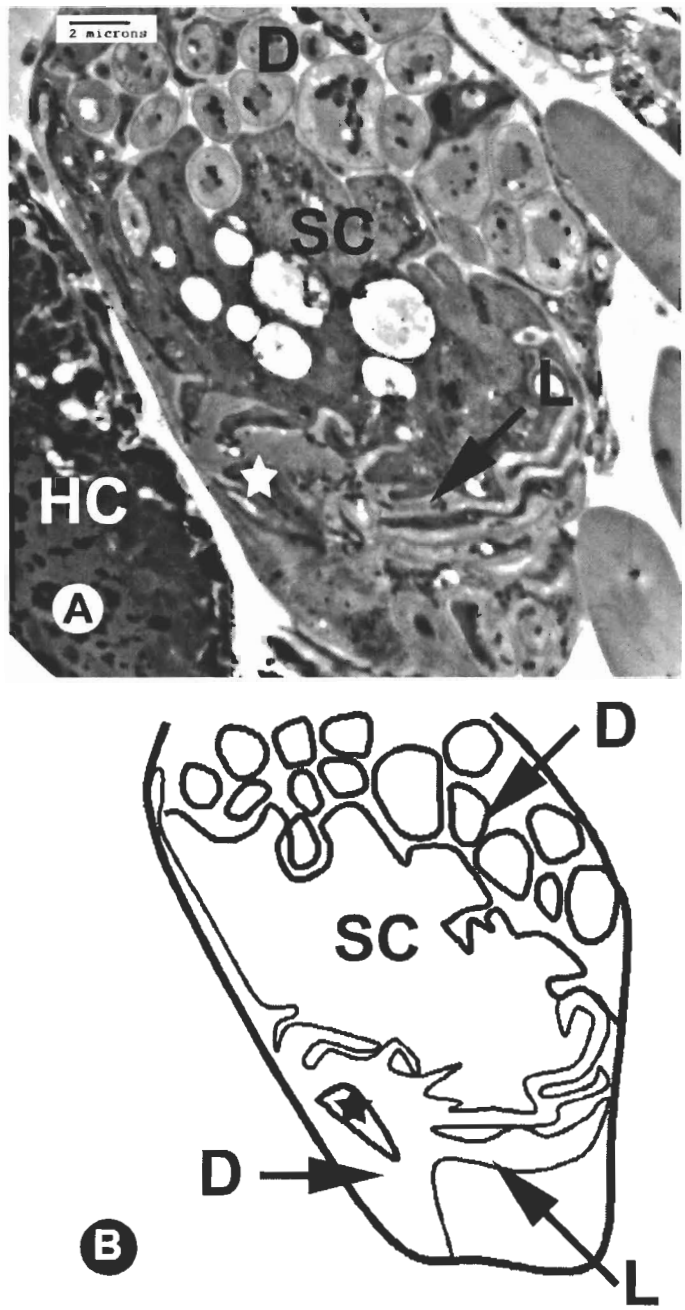

Figure 4. 6. Amphidial track (Preparation #7) at level C (Figure 4. 1) that consists of group of dendrites (D) surrounded with hypodermal cell (HC). (A) TEM. (B) Outline of the dendrites (D) and sheath cell (SC). One of the dendrites (Star) projects a multi-lamellar structure (L) that invaginates the sheath cell.

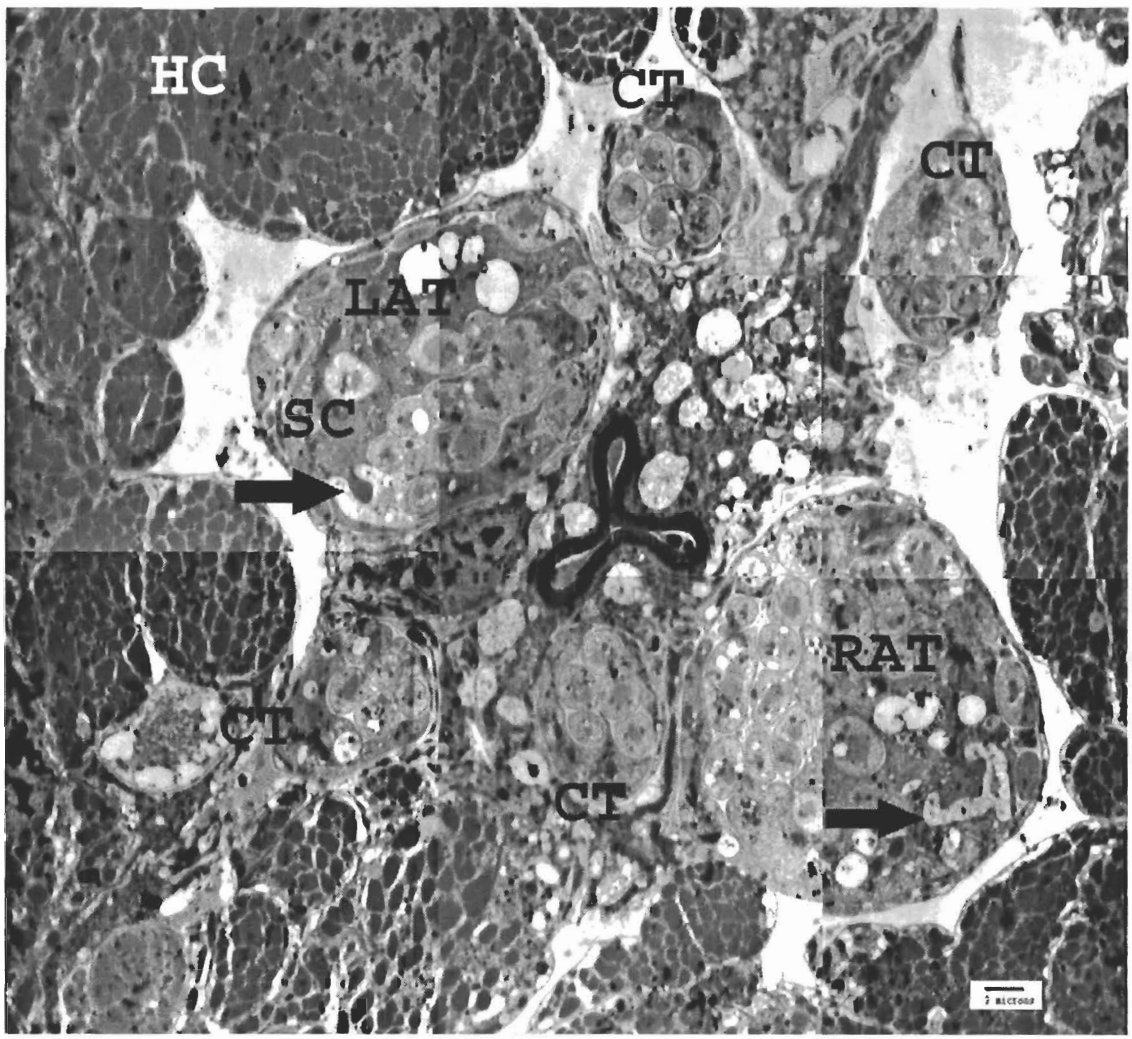

Figure 4. 7. Montaged TEMs of a transverse section at level D (Figure 4. 1) that passes through an amphidial dendrite (Arrows) projecting less extensive lamellae in both left (LAT) and right amphidial tracks (RAT). Note densely packed hemoglobin crystals (cut transversely) in the hypodermal cells (HC). SC, sheath cell; CT, cephalic track.

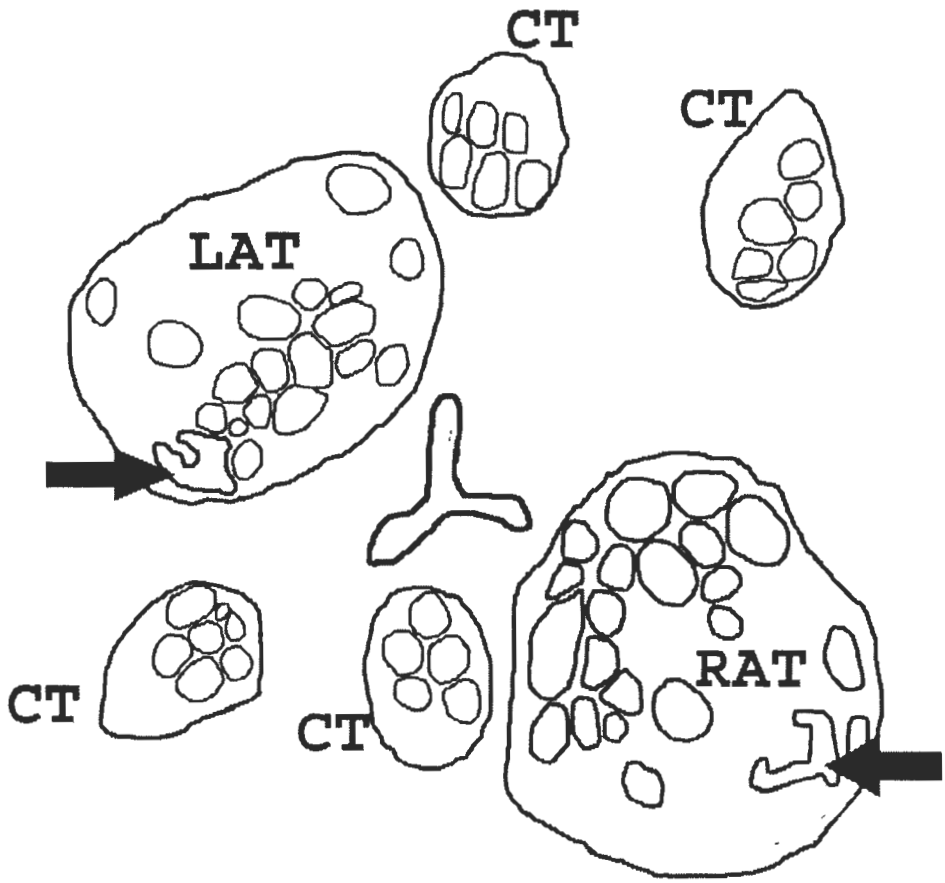

Figure 4. 8. Outline of structures in Figure 4. 7. The lamellar projections (Arrows) in both left (LAT) and right (RAT) amphidial tracks are less extensive at level D. CT, cephalic tracks.

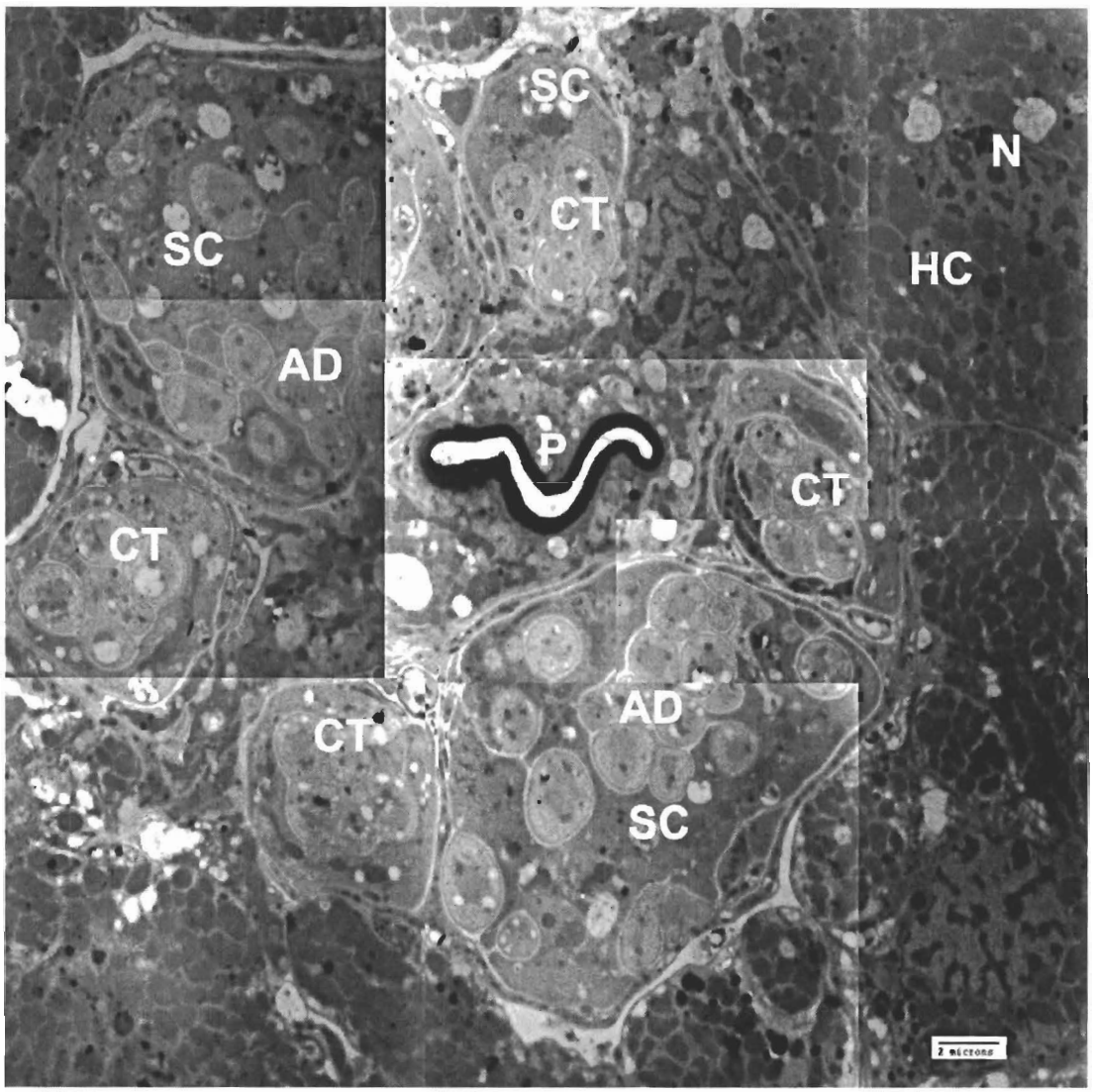

Figure 4. 9. Montaged TEMs of a transverse section posterior to the multilamellar structure (level E in Fig. 4.1). The sheath cell encloses the amphidial dendrites (AD) and the four cephalic tracks (CT). The hypodermal cells (HC) encircle the central sensory neurons and the pharynx (P). N, nucleus.

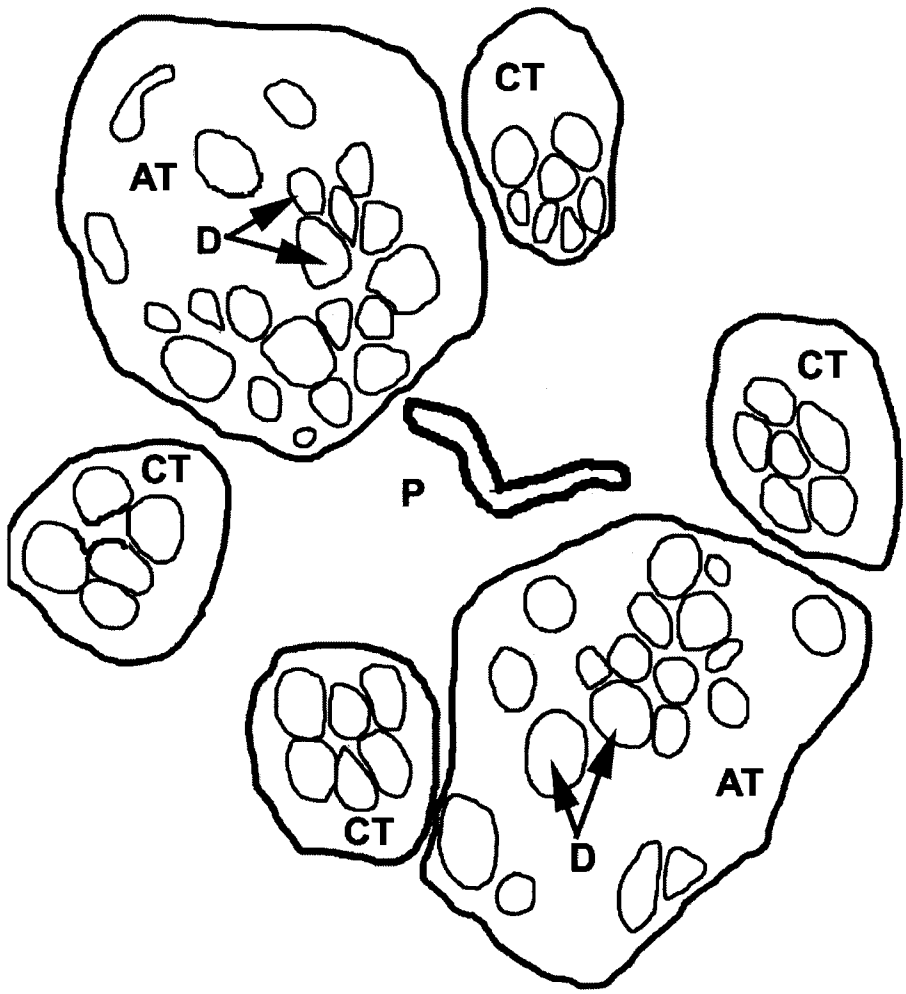

Figure 4. 10. Outlines of structures in Fig 4. 9. AT, amphidial track; CT, cephalic track; D, dendrites; P, pharynx.

Chapter 5
Occurrence of photoreceptors in immature females and J4 juveniles

5.1 Introduction

In chapter 4, serial transmission electron micrographs through the ocellus of the mature female of *M. nigrescens* revealed the presence of a multilamellar dendritic process in the collar region that may be a photoreceptor organelle. This result raised the following question: Are the photoreceptors present in younger stages that lack the shadowing pigment? In this chapter, the objective of the work is to extend these observations to locate multilamellar dendritic processes at different stages of development, namely, the immature female and the fourth stage juvenile. Although both these stages lack the hemoglobin shadowing pigment, they are phototactic. However their phototaxis is weakly negative rather than positive (Burr et al., 2000 a, b).

5.2 Photoreceptors in the immature female

Immature female *M. nigrescens* approximately five months old were investigated. Figure 4.1 B (broken lines) illustrates the location of the transverse sections through the anterior tip of the immature female.

It was observed in a transverse section about 58 μm posterior to the tip and anterior to the collar region that hypodermal cell expansions begin to appear just posterior to the ventrolateral cephalic tracks (Fig. 5.1 A). At 85 μm from the tip the hypodermal expansions encircle most of the pseudocoelom except where the oblique section passes through one

of the amphidial sensilla (Fig. 5.1 B). The photoreceptor lamellae were not observed at this level.

Although at the collar region (Fig. 5.1 C), 105 μm from the tip, the hypodermal expansions entirely encircle the pseudocoelom containing the four cephalic and two amphidial tracks, the multilamellar dendritic processes were not present within the tracks. However, in an oblique transverse section at level D, 110 μm from the tip, lamellae from both of the amphidial dendrites penetrate a sheath cell (Fig. 5.1 D, 5.2, arrows). As for the adult female, the lamellae could be the photoreceptors responsible for the photosensitivity observed in immature females (Burr et al., 2000 a, b). The plasma membranes of photoreceptor lamellae and the sheath cell are closely apposed, which is not the case for the approximately 18 other amphidial dendrites (Figs. 5.3, 5.4, 5.5). As in the mature female, the sheath cell cytoplasm is electron dense (Fig. 5.5).

At a more posterior level, approximately 170 μm from the tip, the sheath cell encircles groups of dendrites that might suggest a specific function for each group (Fig. 5.6). At that level, the dendrite of the multilamellar photoreceptor was difficult to identify from the other dendrites.

The hypodermal cytoplasm appears densely stained in transverse micrographs (Figs. 5.1 B-E, 5.2), which is evidence of a high concentration of protein. In addition, under the light microscope, it was shown that the whole worm has a faint red color of pigment. This pigment was developed in the collar region, and can be distinguished through the worm transparent cuticle. However in electron micrographs, unlike in the adult female, crystals are not present and instead a few dense inclusions with smaller size, 0.1-0.2 μm in diameter, filling the

cytoplasm (Figs. 5.2, 5.12). It is possible that oxyhemoglobin is present in solution but has not reached concentrations where they would form large crystals. Also, accumulation of large vacuoles is evident near the cuticle and the pharynx (Figs. 5.1 B-E, 5.2). Their role is not known.

The hypodermal nucleus occupies approximately 3/4 of its cell diameter (Fig. 5.2). Also, unlike in the adult female (Fig 4.4 inset), the nucleus has a more typical location in the center (5.2, 5.12 A). In posterior micrograph at 122μm from the tip, level E, the hypodermal cells divide the muscle into six bands (Fig. 5.1 E).

5.3 Comparative anterior morphology of J4 juveniles

After 4-5 weeks of infection, J4 female juveniles were fixed for TEM on the same day of emergence. Figure 5.7 illustrates the anterior anatomy of the J4 that differs significantly from that of the immature and mature adult stages. The J4 cuticle is about 16 μm in thickness in the anterior (Fig 5.8), which is slightly thinner than that of the adult (Table 3). The J4 is distinguished by not having a collar of thickened cuticle (28 μm).

Another difference is that under the light microscope there is no evidence for developing a faint red color yet. In electron micrographs, the hypodermal cell cytoplasm is not as densely stained in J4 as in immature female, however it does contain small inclusions that could be hemoglobin crystals (Fig. 5.12 B). In transverse light micrographs, the hypodermal cells begin at about 95 μm from the tip to encircle the pseudocoelom just posterior to the sensory tracks (Fig. 5.8 D). At 135 μm from the tip, the hypodermal cells divide the muscle into six bands (not shown).

The morphology and arrangement of the sensilla in J4 are similar to those in the adult and immature female. In J4, two dorsolateral and two ventrolateral cephalic sensilla are located 46 μm from the tip (Fig. 5.8 A, B), and two lateral amphidial sensilla are located at 64 μm from the tip (Fig. 5.8 C). Each sensillum consists of a sheath cell and dendritic processes that connect to dendrites at about 95 μm. These dendrites are segregated into tracks that extend posteriorly along side of the pharynx (Fig. 5.8 D-F).

5.4 Photoreceptors in the J4 juveniles

Figure 5.7 illustrates the location of the transverse sections through the anterior tip of J4.

Oblique transverse section at level B2, about 95 μm posterior to the tip, shows that the right amphidial track has just entered the sensillum (Fig. 5.8 D). In electron micrographs at this level and at 105 μm from the anterior, the more posteriorly sectioned left amphidial track, there is no evidence of a multilamellar dendritic process (Fig. 5.9 A, B). From level B2 to level C, the amphidial track consists of only a sheath cell surrounding groups of dendrites which are observed to end anteriorly within the sensillum and are presumed to be chemoreceptor neurons as for *C. elegans* (Ward et al., 1975; Albert and Riddle, 1983; Bargmann et al., 1993)

However, at level C (Fig. 5.8 E) about 110 μm posterior to the tip, multilamellar dendritic processes invaginate the sheath cell in both the left and right amphidial tracks (Fig. 5.10). As for the adult female and immature female, the lamellae could be the photoreceptors responsible for the photosensitivity observed in J4 (Burr et al. 2000 a, b). At a more

posterior level about 117 μm from the tip, multilamellar structures are located ventrolaterally in both tracks and are surrounded with the hypodermal expansions (Fig. 5.11). The continuous sheath cell separates the lamellae from the other 18 dendrites.

5.5 Conclusions

5.5.1 Comparison with adult female

Similar to the adult female, multilamellar dendritic processes invaginate the sheath cell in both amphidial tracks in the collar region of the immature female and in an equivalent position 110 μm posterior to the tip in J4. In both immature and J4, the multilamellar processes terminate anteriorly at 105 μm (Figs. 5.1 C, 5.9). The location of the lamellar dendritic processes, their ventrolateral position in each amphidial track, invagination of the sheath cell and position relative to the cylinder-shaped projections of the hypodermal cords, lead to the conclusion that the lamellae are the same structure in the three life stages, and as in the mature adult female, could be photoreceptor organelles. In addition, the observation of photoreceptor structures is consistent with the light sensitivity of the immature and J4 females (Burr et al., 2000 a, b).

5.5.2 Implications for photoreceptor development

The multilamellar photoreceptors may develop in *Mermis* during the J4 stage. In J4, the dendritic processes have less extensive lamellae than in the immature female or adult female. The developmental result is

generally agrees with those described by (Chalfie and white, 1988) who reported that during the development of the nervous system of the nematode *C. elegans* from larva to adult, some neurons may develop early yet mature late.

The developmentally associated changes in other nematode photoreceptors are still unknown. However, changes in photoreceptor sensitivity to flickering light have been described in developing zebrafish (Branchek, 1984).

5.5.3 Implication for behavior

Electron microscopic examination of the hypodermal cells in both immature female and juvenile revealed an internal morphology unlike that of the mature female. The hypodermal cytoplasm contains less dense inclusions of protein and a nucleus occupying 3/4 of the cell diameter (Fig. 5.12). This corresponds with the absence of hemoglobin pigmentation in J4's and faint color in the 5 month old immature females that were examined. Burr et al. (2000 b) suggested that when the anterior is oriented away from the light of J4 and immature females, the body posterior to the photoreceptor would shade the photoreceptor and thus provide the signal necessary for the observed negative phototaxis.

This is similar to the shadowing arrangement in *O. vesicarius,* in which the eyespots posterior to the photoreceptors would shade the photoreceptor from light coming from the posterior hemisphere (Burr and Burr, 1975). Therefore, it is possible that in *Mermis*, accumulation of enough oxyhemoglobin pigment to shade the photoreceptors could account for the switch to positive phototaxis in the adult. In the mature

Mermis, the cytoplasm oxyhemoglobin crystals occupy more than 1/2 the volume of the hypodermal cells (Fig 4.4) encircling the photoreceptors.

Figure 5. 1. Morphology of an immature female. Light micrographs of somewhat oblique transverse semi-thick sections at different levels through the anterior (Broken lines in Figure 4.1): A, B. Sections through different levels of the sensilla. (A) Section 58 μm from tip (level B, Fig. 4.1), that passes through the two dorsolateral cephalic sensilla (CS), the two ventrolateral cephalic tracks (CT), and the lateral amphidial sensilla (AS) at different levels. (B) Section 85 μm from the tip (Fig. 4.1, level between B and C) that passes through the four cephalic tracks (CT), one amphidial sensillum (AS) and one amphidial track (AT). N, nucleus of hypodermal cell.

C, D. Sections through the collar region. (C) Section 105 µm from the tip (Fig. 4.1, level C) that passes through the hypodermal cells (HC) surrounding two amphidial tracks (AT) and four cephalic tracks (CT). Note the thickness of the cuticle (C). (D) Section 110 µm from the tip (Fig. 4.1, level D) that passes through the multi-lamellar dendritic process (arrows) in the two lateral amphidial tracks (AT).

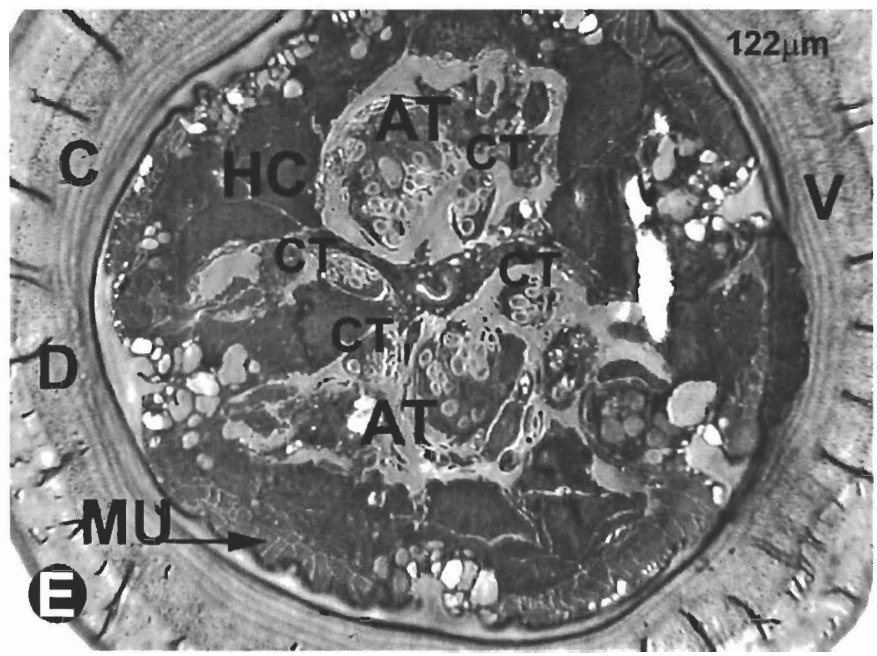

E. Section 122µm from the tip (Fig. 4.1, level E) at the level of the appearance of the muscle bands (MU). D, dorsal side; V, ventral side; HC, hypodermal cells; C, cuticle; CT, cephalic track.

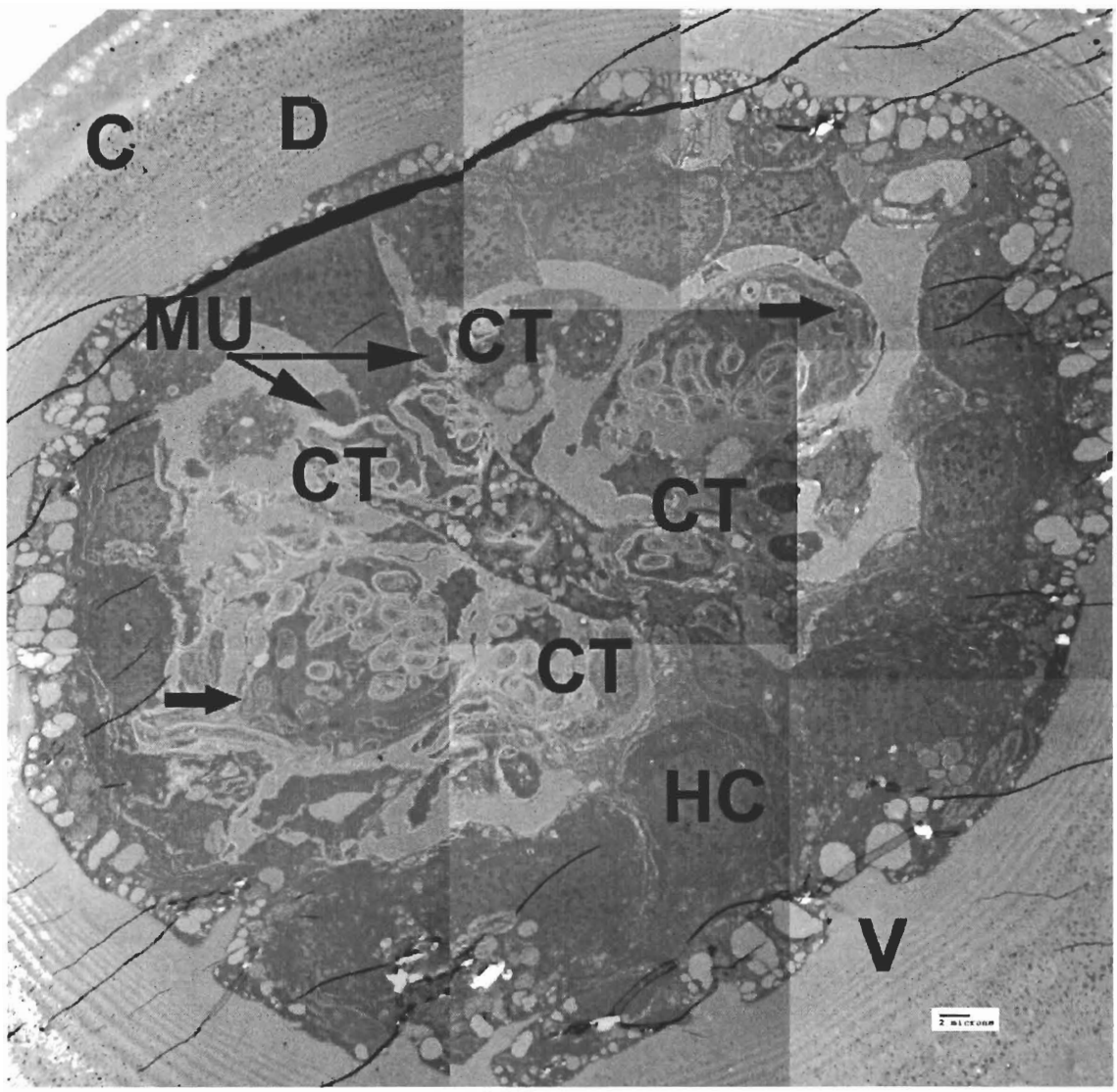

Figure 5.2. Immature female. Montaged TEMs of a section in the collar region (110 μm from the tip) (level D, Fig. 4.1) that passes through multilamellar dendritic process (Arrows). The hypodermal cells (HC) encircle the four cephalic tracks (CT), and the two lateral amphidial tracks. C, cuticle; D, dorsal side; V, ventral side; MU, muscle bands in the pseudo-coelom.

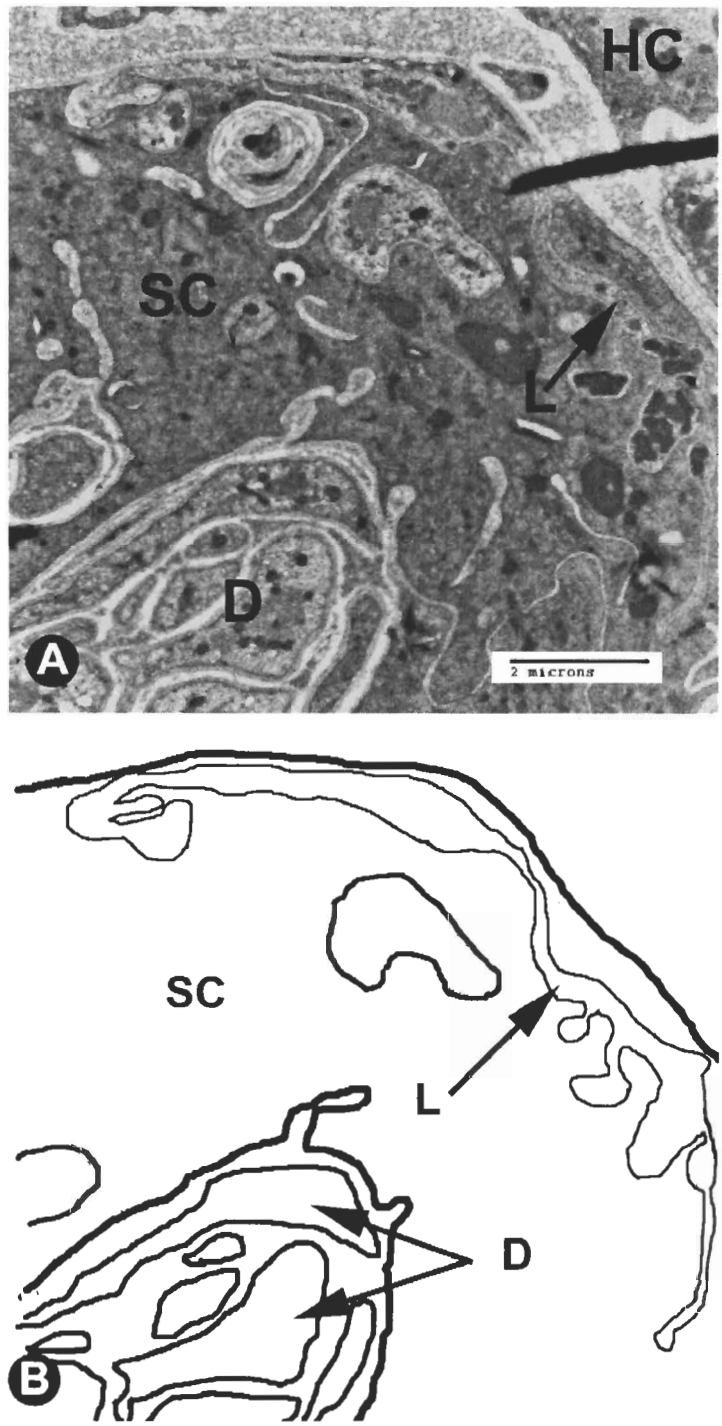

Figure 5.3. Immature female. Section 110 m from tip (level D, Fig. 4.1). Enlargement of Fig. 5.2, right-hand amphidial track. (A) A multilamellar dendritic process (L) invaginating the sheath cell (SC) that encircles a group of dendrites (D). HC, hypodermal cell. (B) Outlines of structures in A.

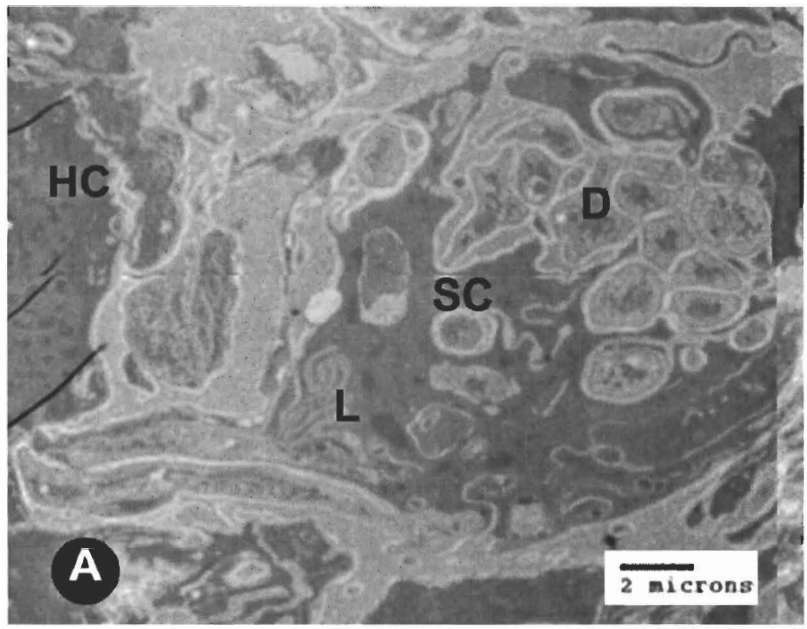

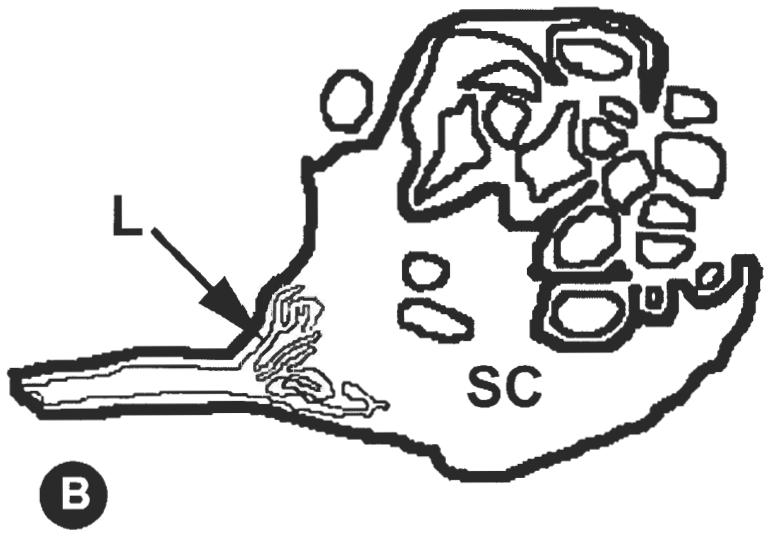

Figure 5.4. Immature female. Oblique section 110 m from tip (level D, Fig. 4.1). Enlargement of Fig. 5.2, left-hand amphidial track. (A) A multi-lamellar dendritic process (L) projecting into the sheath cell (SC) that surrounds the eighteen amphidial dendrites (D). HC, hypodermal cell. (B) Outlines of structures in A.

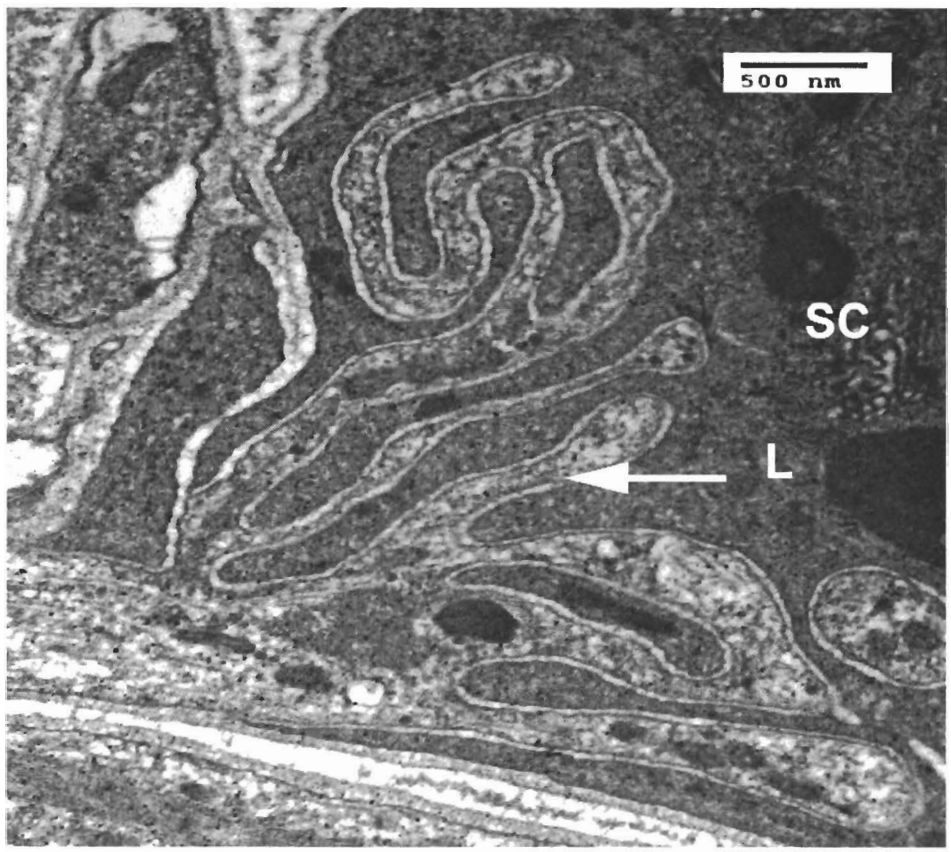

Figure 5. 5. Enlargement of multilamellar dendritic process in Fig. 5.4 .The lamellae (L) invaginate the sheath cell (SC).

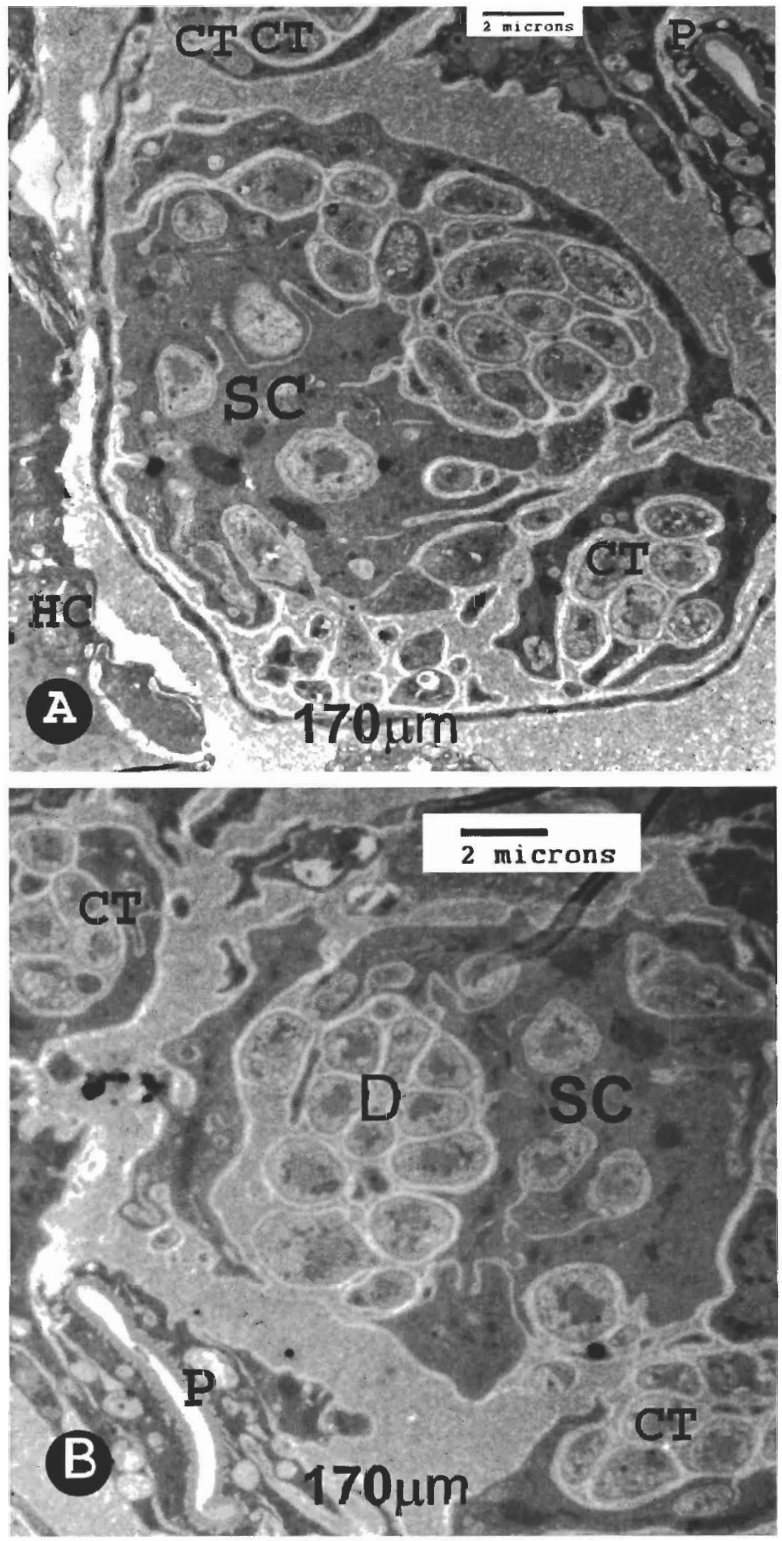

Figure 5.6. Immature female. Section 170 µm from tip (level E, Fig. 4.1) that passes posterior to the multi-lamellar dendrite processes. (A) Right amphidial track. (B) Left amphidial track. The sheath cell (SC) fills most of the track area and encircles groups of amphidial dendrites. CT, cephalic track; P, pharynx; HC, hypodermal cells.

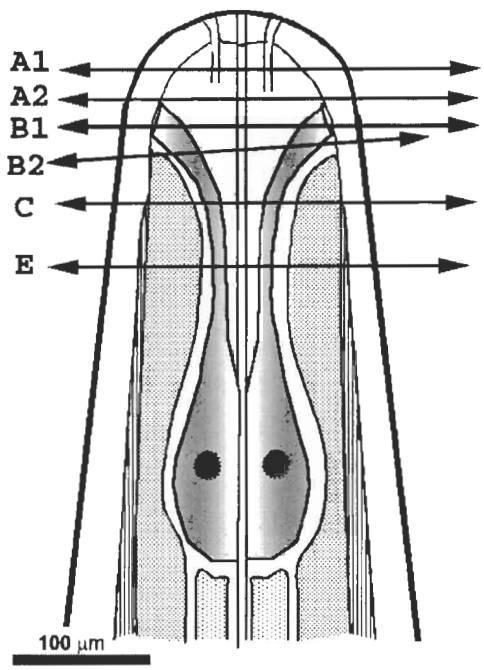

Figure 5.7. Anterior tip of a fourth stage larva of *Mermis nigrescens*. Longitudinal section through the midline and dorsal view illustrating the location of the transverse sections to be illustrated in subsequent figures.

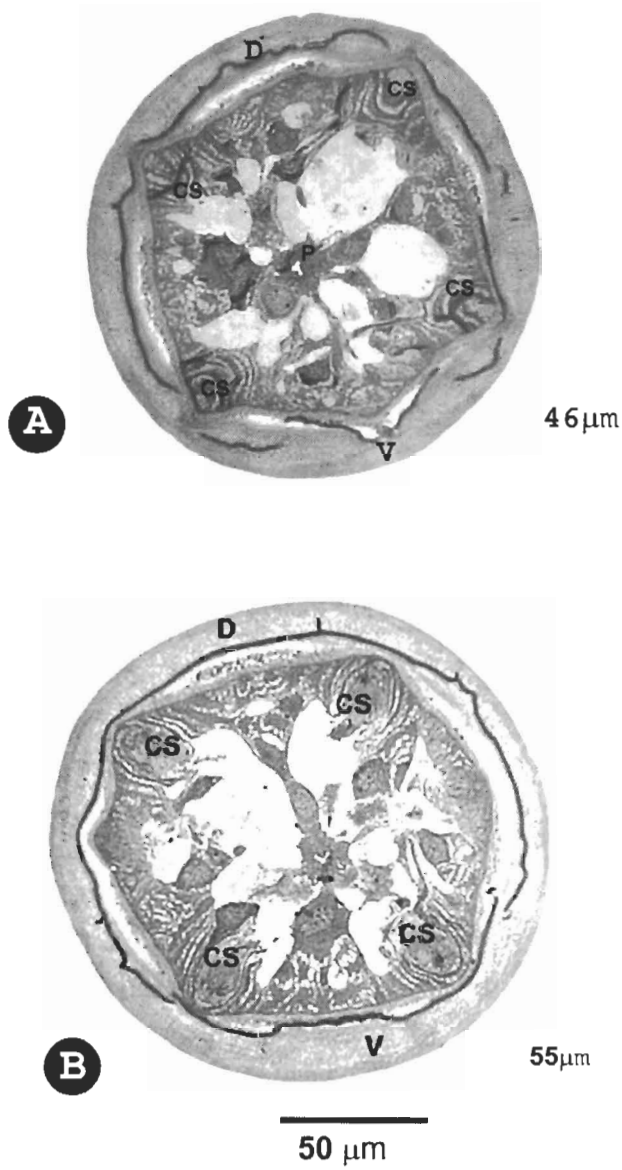

Figure 5.8. Morphology of a fourth stage female larva. Light micrographs of transverse semi-thick sections at different levels through the anterior:

A, B. Sections at different levels of the anterior sensilla. A) Near the tip, at 46 μm (Fig. 5.7, level A1) through the four cephalic sensilla (CS). (B) Section at 55 μm from tip (level A2, Fig. 5.7) that passes through the four cephalic sensilla (CS) and just anterior to the lateral amphidial sensilla.

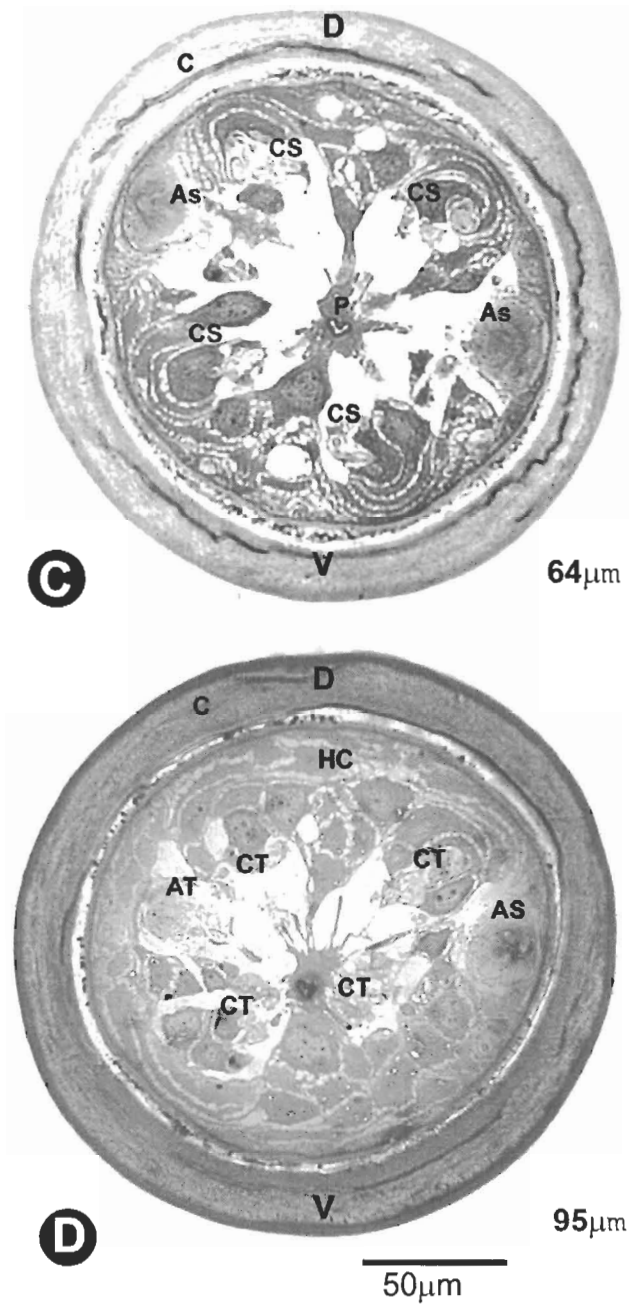

C, D. Sections through different levels of the sensilla and tracks. (C) Section at 64 μm from tip through the four cephalic sensilla (CS) and two lateral amphidial sensilla (AS) (Fig. 5. 7, level B1). (D) Oblique section at 95 μm from tip (Fig 5.7, at level B2) through amphidial sensillum (AS) and amphidial track (AT). Hypodermal cells (HC) surround the cephalic tracks (CT). D, dorsal; V, ventral; C, cuticle.

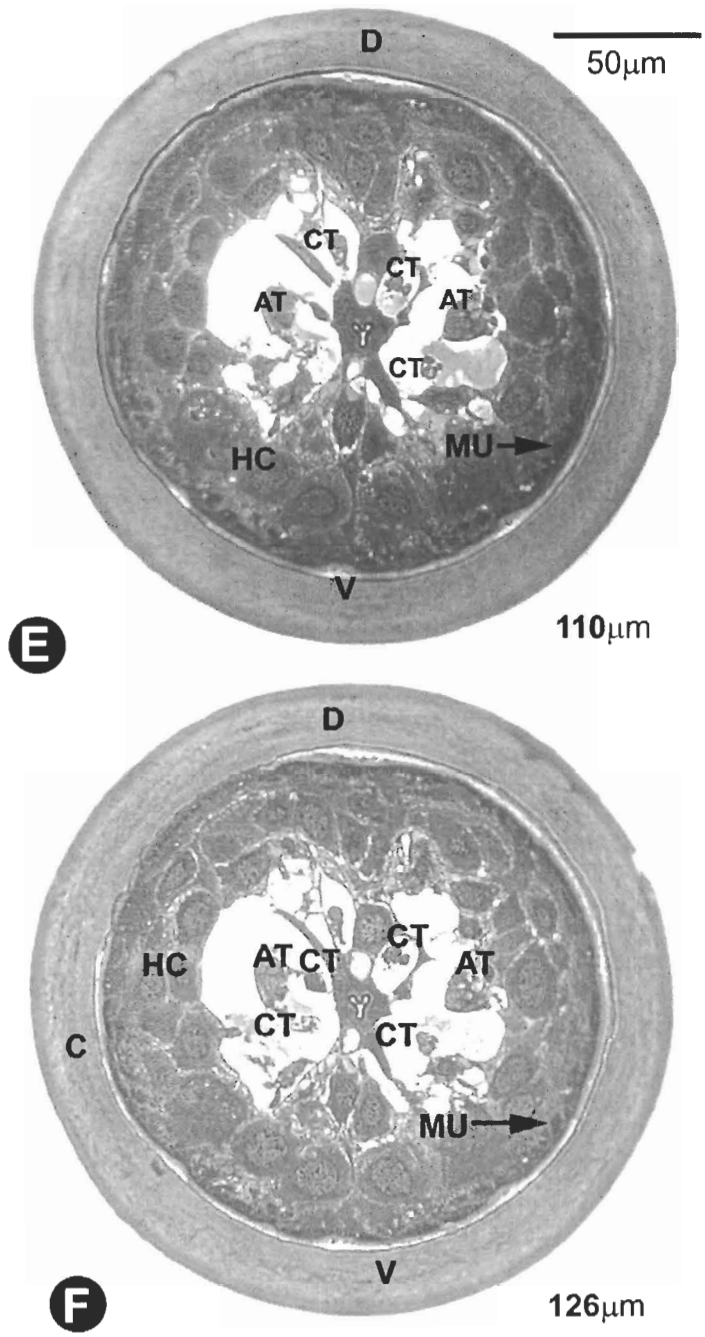

E, F. Sections through the hypodermal expantions. (E) Section at 110 μm from tip (level C, Fig. 5.7) that passes at the appearance of the muscle (MU). The hypodermal cells (HC) encircle the four cephalic tracks (CT) and two lateral amphidial tracks (AT). (F) Section at level D (Fig. 5.7) that shows muscle spindles that have consistent thickness (MU). D, dorsal side; V, ventral side; C, cuticle.

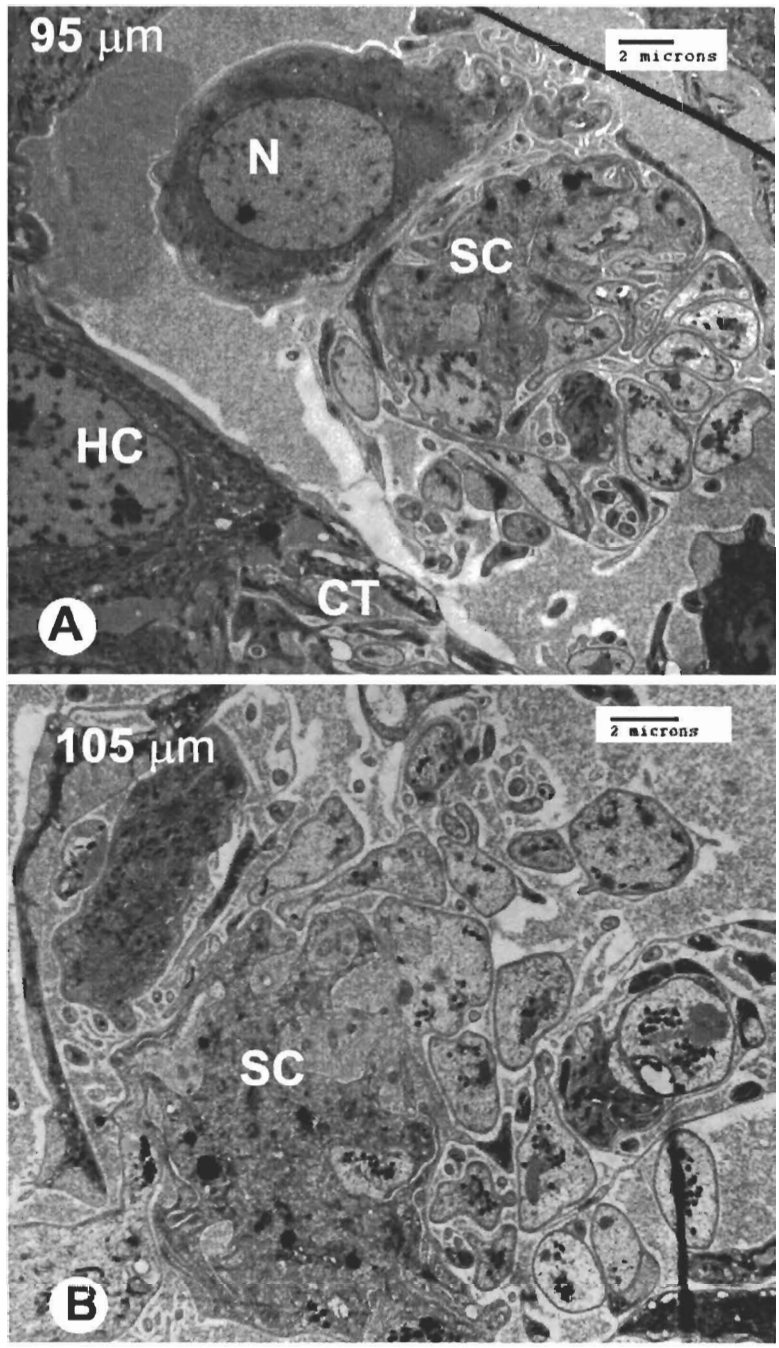

Figure 5. 9. TEMs through the left amphidial track at different level s: (A) At 95 μm from the tip (Level B2, Fig. 5. 7), the amphidial track is surrounded with hypodermal cells (HC) and has a prominent sheath cell (SC). (B) At 105 μm from tip, (between B2 and C, Fig. 5. 7) the sheath cell (SC) surrounds dendrites that are somewhat larger than immature female.. N, nucleus; CT, cephalic track.

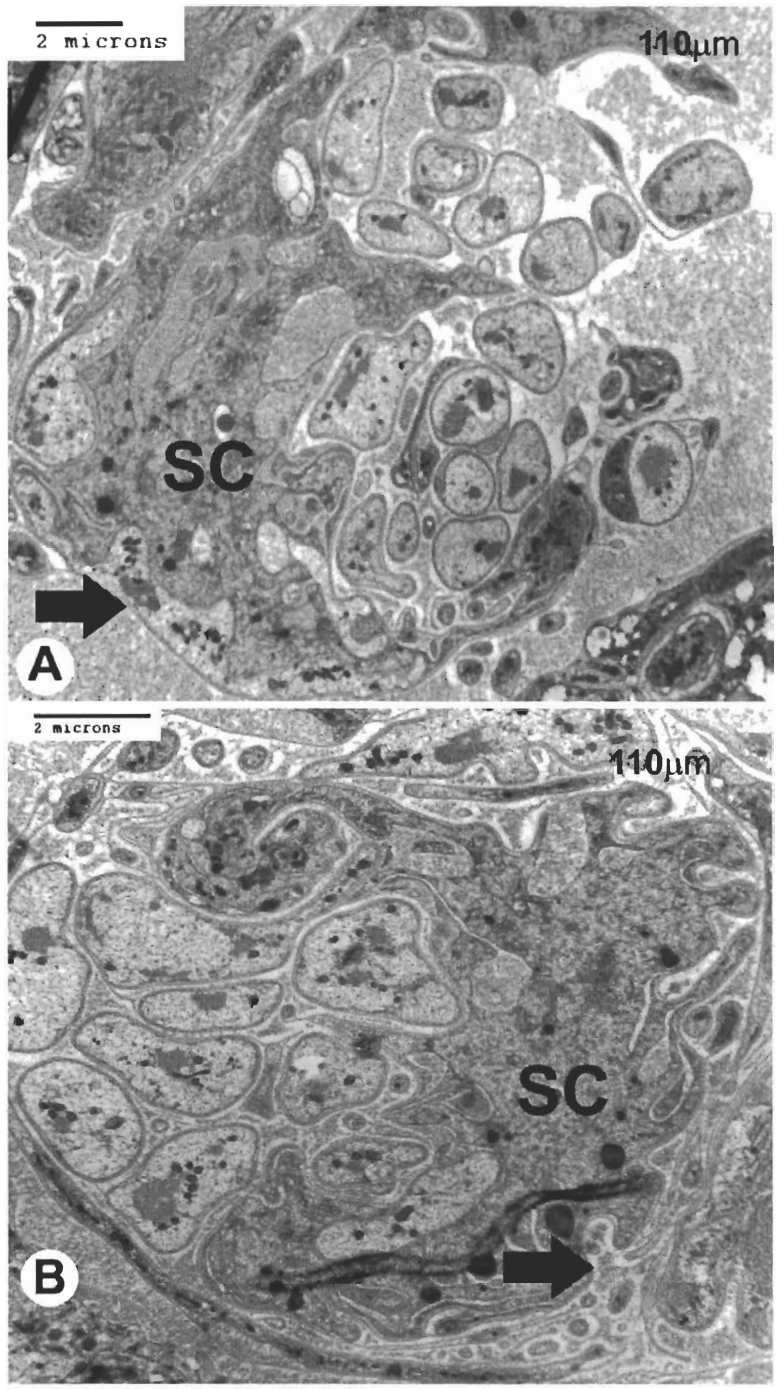

Figure 5.10. Amphidial tracks of L4 larva at 110 µm from the tip (Fig. 5.7, level C). (A) In the left track, the multilamellar dendritic process (Arrow) is separated by a sheath cell (SC) from groups of dendrites. (B) In the right amphidial track, similar structure (Arrow).

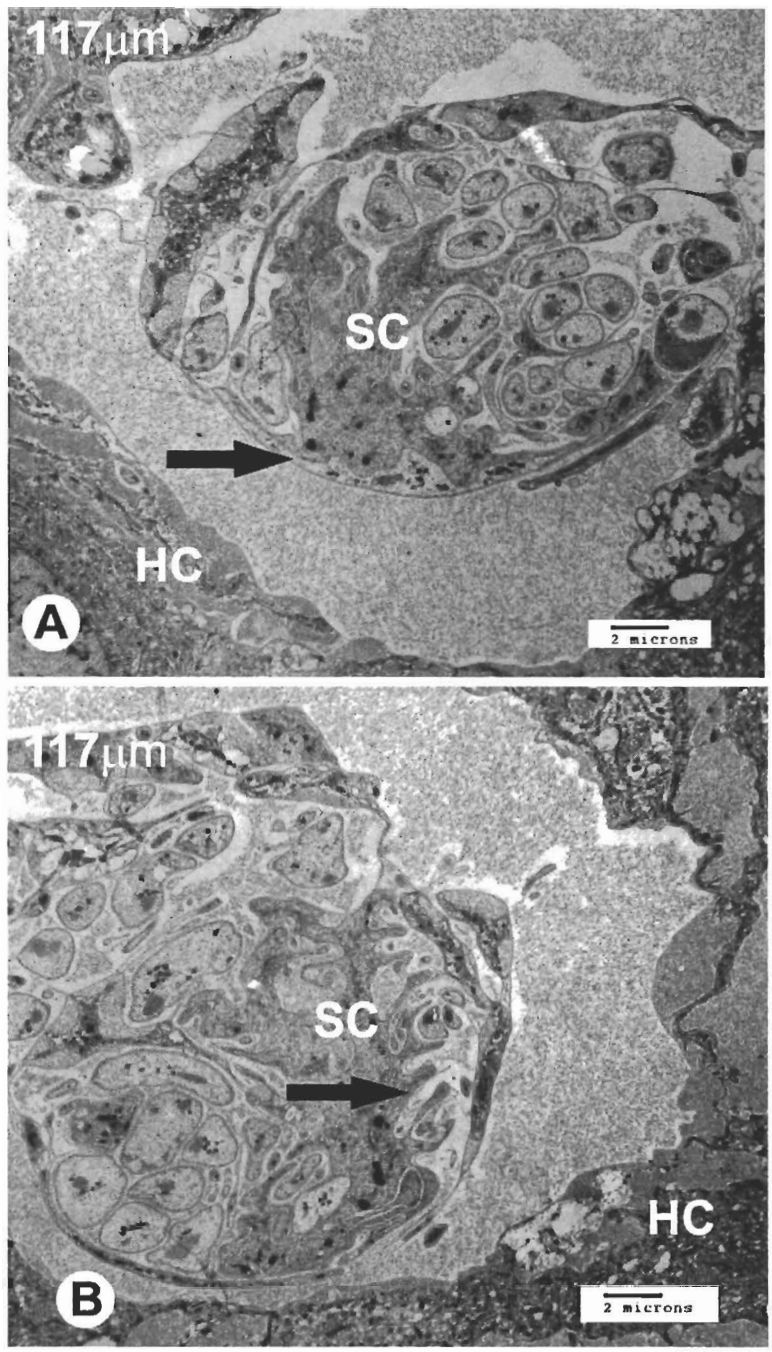

Figure 5. 11. Amphidial tracks at 117 μm from tip (Fig. 5.7, level between C and D) surrounded with the hypodermal cell (HC). (A) In the left amphidial track, the sheath cell (SC) fills most of the track area and encircles a ventro-lateral lamellar dendritic process (Arrow) and groups of amphidial dendrites. (B) In the right amphidial track, the multilamellar dendritic process (Arrow) invaginates the sheath cell (SC).

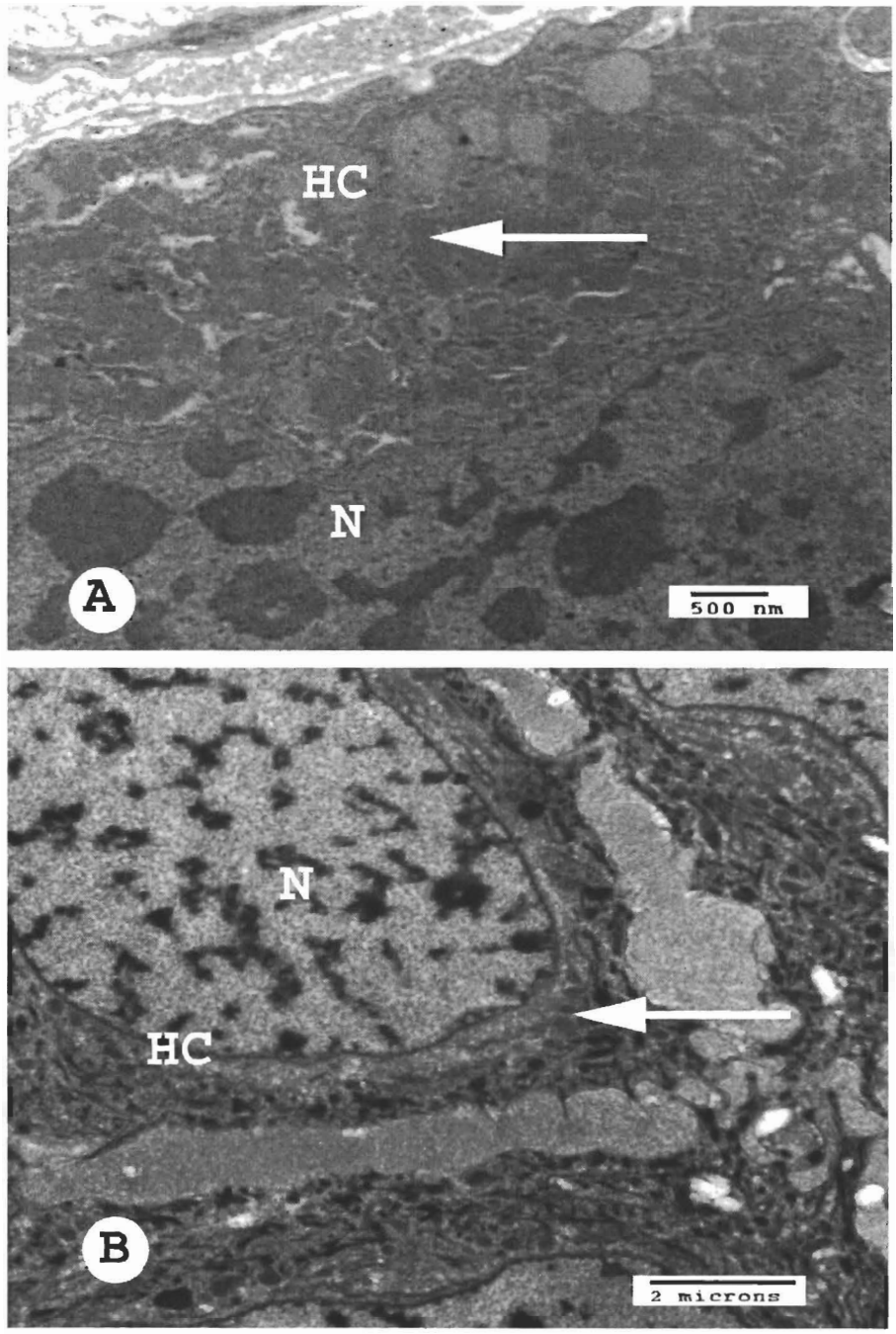

Figure 5.12. Hypodermal cells (HC) containing large nucleus (N) and cytoplasm filled with dense inclusions (Arrows). (A) Immature female (B) Fourth stage larva.

Chapter 6
Summary and Conclusion

The main objectives of the thesis were to locate the photoreceptors of the mature female *Mermis nigrescens*, to describe their structure and to compare the photoreceptors with other sensory structures in the nematode. The comparison was intended to distinguish them as photoreceptors. Additional objectives were to investigate the occurrence of the photoreceptor in the immature female and fourth stage juvenile and to improved fixation and embedding techniques for *Mermis*.

6.1 Identification and localization of the photoreceptor

Both light and transmission electron microscopes (TEM) were used to analyze the morphology, fine structure and location of the ocellus of the mature *Mermis*. It was possible to locate a dendrite in each amphidial track that projects lamellae into the sheath cell. This multilamellar dendritic process is the most likely candidate for the photoreceptor based on its morphology, fine structure and location.

6.1.1 Morphology and fine structure

The morphological reasons for hypothesizing that the multilamellar dendritic processes are photoreceptors can be summarized as follows.

- The invagination of the sheath cell by the lamellae and the close apposition of the lamellae with the sheath cell membrane identify the multilamellar dendritic process as a sensory organelle.
- The non-ciliary structure distinguishes the multilamellar receptors from the ciliary chemoreceptors at the distal end of the amphids.

- Their very different fine structure and their location distant from the cuticle distinguish them from mechanoreceptors.
- The expansion of membrane surface area as multiple lamellae is a feature of epigenetic photoreceptor organelles found in nematodes and other animals.
- Further, the orientation of the lamellae perpendicular to the direction of light is characteristic of photoreceptor organelles, as this can increase their light sensitivity.

6.1.2 Location

Further evidence that the multilamellar dendritic processes may be a photoreceptor is provided by their location.

- They are the only sensory neurons appearing in this region.
- Their remote location approximately 20 um from the amphidial channel and deep within the body, unlike the wing chemoreceptors of the *C. elegans* amphid, suggests further that the multilamellar dendritic process has a function other than chemosensation.
- Similar to photoreceptors in ocelli of nematodes and other animals, the multilamellar projections are located so that they would be effectively shadowed except from a narrow range of directions. The photoreceptors must be so located to provide the *Mermis* with its directional sensitivity towards light.
- Photoreceptors located within the cylinder of pigment were required by the results of behavioral experiments (Burr and Babinszki, 1990).

In conclusion, based on arguments from their morphology, fine structure and location, the multilamellar dendritic processes are most

likely to be the photoreceptors required for phototaxis of *Mermis nigrescens*.

6.2 Photoreceptors in younger stages

The location of the multilamellar processes in the immature female and J4 was similar to that in mature females. In the immature female, the lamellar dendrites were observed at the collar region, as in the mature female, and they were located in an equivalent position 110 μm from the tip in the juvenile J4, which lack the cuticular collar.

6.3 Photoreceptor evolution

One of the dendrites in the amphidial track forms the lamellae and ends within the ocellus rather than continuing anteriorly to the amphidial sensillum where the other dendrites have a chemosensory function. This indicates that the multilamellar dendritic process might have evolved for photoreception from one of the amphidial chemoreceptor neurons.

6.4 Development of eye structure

Comparative analysis of the fine structure of the hypodermal cells of the mature worm showed that the cytoplasm is packed with hemoglobin crystals with a diameter of 0.3-1.0 μm. The nucleus is dislocated to the cell's periphery. In case of J4 and immature female, the hypodermal cytoplasm has fewer dense inclusions with smaller diameter 0.1-0.2 μm. Therefore, it could be concluded that the alteration in the structural morphology of the hypodermal cells is attributed to the

alteration in photobehavior. The lamellar organelle has less extensive lamellae in the emergent J4 juveniles, suggesting that the photoreceptor organelle develops during the J4 stage.

6.5 Ultrastructure preparation technique

In order to investigate the photoreceptor morphology, an optimal method for preparing the nematode *M. nigrescens* for ultra-structural study was developed. In this preparation, uranyl acetate *en bloc* staining after osmication was used. Results showed improved membrane fixation, well-preserved cytoskeletal myofilaments of muscles and, well-fixed neuron microtubules.

References

Albert, P. S., Riddle, D. L. (1983). Developmental alteration in sensory neuroanatomy of the *Caenorhabditis elegans* dauer larva. J. Comp. Neurol. 219: 461-481.

Arnheiter, H. (1998). Eyes viewed from the skin. Nature 391: 632-633.

Ashton, F.T., Li, J. and Schad, G.A. (1999). Chemo- and thermosensory neurons: structure and function in animal parasitic nematodes. Vet. Parasitol. 84: 297-316.

Baker, G. L., and Capinera, J. L. (1997). Nematodes and nematomorphs as control agents of grasshoppers and locusts. Memoirs Entomol. Soc. Can. 171: 157-211.

Bargmann, C. I., Hartwieg, E., and Horvitz, H. R. Odorant-selective genes and neurons mediate olfaction in *C. elegans*. Cell 74: 515-527.

Batson, B. S. (1979). Body wall of juvenile and adult *Gastromermis boophthorae* (Nematoda: Mermithidae): ultrastructure and nutritional role. Int. J. Parasitol. 9: 495-503.

Bollerup, G. and Burr, A. H. (1979). Eyespots and other pigments in nematode esophagus muscle cells. Can. J. Zool. 57: 1057-1069.

Branchek, T. (1984). The development of photoreceptors in the Zebrafish, Brachydanio rerio. II. Function. J. Comp. Neuro. 224: 116-122.

Burr A. H. (1984). Evolution of eyes and photoreceptor organelles on the lower phyla. In: Photoreception and Vision in Invertebrates. Edited by M.A. Ali, pp.131-178. New York, Plenum Press

Burr A. H. (1985). The photomovement of *Caenorhabditis elegans*, a nematode which lacks ocelli. Proof that the response is to light not radiant heating. Photchem. Photobiol. 41: 577-582.

Burr, A. H. J. and Babinszki, C. P. F. (1990). Scanning motion, ocellar morphology and orientation mechanisms in the phototaxis of the nematode *Mermis nigrescens*. J. Compar. Physiol. A 167: 257-268.

Burr, A. H. J., Babinszki, C. P. F., and Ward, A. J. (1990). Components of phototaxis of the nematode *Mermis nigrescens*. J. Comp. Physiol. A 167: 245-255.

Burr, A. H. and Burr, C. (1975). The amphid of the nematode *Oncholaimus vesicarius*: ultrastructural evidence for a dual function as chemoreceptor and photoreceptor. J. Ultrastruct. Res. 51: 1-15.

Burr, A. H. J., Eggleton, D.K., Patterson, R. and Leutscher-Hazelhoff, J.T. (1989). The role of hemoglobin in the phototaxis of the nematode *Mermis nigrescens*. Photochem. Photobiol. 49: 89-95.

Burr, A. H. J. and Gans, C. (1998). Mechanical significance of obliquely striated architecture in nematode muscle. Biol. Bull. 194: 1-6.

Burr, A. H. and Harosi, F. I. (1985). Naturally crystalline hemoglobin of the nematode *Mermis nigrescens*. Biophys J. 47: 527-536.

Burr, A. H. J., Hunt, P., Wagar, D. R., Dewilde, S., Blaxter, M. L., Vanfleteren, J. R. and Moens, L. (2000a). A hemoglobin with an optical function. J. Biol. Chem. 275: 4810-4815.

Burr, A. H. J., Wagar, D. and Sidhu, P. (2000b). Ocellar pigmentation and phototaxis in the nematode *Mermis nigrescens*: changes during development. J. Exper. Biol. 203: 1341-1350.

Burr, A. H. and Webster J. M. (1971). Morphology of the eyespot and description of two pigment granules in the esophageal muscle of a marine nematode, *Oncholaimus vesicarius*. J. Ultrastruct. Res. 36: 621-632.

Chalfie, M. and Au, M. (1989). Genetic control of differentiation of the *Caenorhabditis elegans* touch receptor neurons. Science 24: 1027-1033.

Chalfie, M. and Thomson, J. N. (1982). Structural and functional diversity in the neuronal microtubules of *Caenorhabditis elegans*. J. Cell Biol. 93: 15-23.

Chalfie, M and White, J. (1988). The nervous system. In: *The Nematode* Caenorhabdities elegans. Edited by W. B. Wood, pp. 337-391.Cold spring Harbor laboratory.

Christie, J. R. (1937). *Mermis subnigrescens*, a nematode parasite of grasshoppers. J. Agric. Res. 55: 353-364.

Cobb, N. A. (1926). The species of *Mermis*. J. Parasitol. 8: 66-72.

Coomans, A. (1979). The anterior sensilla of nematodes. Revue Nematol. 2: 295-283.

Craig, S. M. and Webster, J. M. (1978). Viability and hatching of *Mermis nigrescens* eggs and subsequent larval penetration of the desert locust, *Schistocerca gregaria*. Nematologica 24: 472-473.

Croll, N. A., Evans, A. A. F. and Smith, J. M. (1975). Comparative nematode photoreceptors. Comp. Biochem. Physiol. 51A: 139-143.

Croll, N. A., Riding, I. L. and Smith, J.M. (1972). A nematode photoreceptor. Comp. Biochem. Physiol. 42A: 999-1009.

Deininger, W., Fuhrmann, M. and Hegemann, P. (2000). Opsin evolution: out of wild green yonder? Trends in Genetics 16: 158-159.

Eakin, R. M. (1968). Evolution of photoreceptors. In: Evolutionary Biology, Vol. II , edited by T. Dobzhansky, M.K. Heckt and W.C. Streere. pp. 194-242. Appleton-Century-Crofts, New York.

Eakin, R. M. (1972). Structure of invertebrate photoreceptors. In: Handbook of Sensory Physiology. Vol. VII/1, edited by H.J.A. Dartnall. pp. 625-684. Springer-Verlag, Berlin.

Eakin, R. M. (1982). Continuity and diversity in photoreceptors. In: Visual Cells in Evolution. Edited by. J.A.Westfall. pp. 91-105. New York, Raven Press

Ellenby, C. (1964). Haemoglobin in the chromatrope of an insect parasitic nematode. Nature 202: 615-616.

Ellenby, C. and Smith, L. (1966). Hemoglobin in *Mermis subnigrescens* (Cobb), *Enoplus brevis* (Bastian) and *E. communis* (Bastian). Comp. Biochem. Physiol. 19: 871-877.

Endo, B. Y. (1980). Ultrastructure of the anterior neurosensory organs of the larvae of the soybeans cyst nematode *Heterodera glycines*. J. Ultrastruct. Res. 72: 349-366.

Gans, C. and Burr, J. (1994). Unique locomotory mechanism of *Mermis nigrescens* a large nematode that crawls over soil and climbs through vegetation. J. Morphol. 222: 133-148.

Giammara, B. L. (1993). Microwave embedment for light and electron microscopy using epoxy resin, LR white, and other polymers. Scanning 15: 82-87.

Godement, P. Vanselow, J., Thanos, S. and Bonhoeffer, F. (1987). A study in developing visual system with a new method of staining neurons and their processes in fixed tissues. Development 161: 697-713.

Hall, D. H. (1995). Electron microscopy and three dimensional reconstruction. Meth. Cell Biol. 48: 395-436.

Hayat, M. A. (2000). Principles and techniques of electron microscopy. Biological applications. Cambridge University Press.

Hedgecock, E. M., Culotti, J. G., Thomson, N., Perkins, L. A. (1985). Axonal guidance mutants of *Caenorhabditis elegans* identified by filing sensory neurons with fluorescein dyes. Devel. Biol. 111: 158-170.

Hegemann, P., Fuhrmann, M. and Kateriya, S. (2001). Algal sensory photoreceptors. J. Phycol. 37: 668-676.

Insausti, T. C. and Lazzari, C. R. (2002). The fine structure of the ocelli of *Triatoma infestans* (Hemiptera: Reduviidae). Tissue and Cell 34: 437-449.

Jones, J. (2002). Nematode sense organs. In: The Biology of Nematodes. Edited by D.L. Lee. pp 353-366. London.

Karnovsky, M. J. (1965). A formaldehyde-glutaraldehyde fixative of high osmolarity for use in electron microscopy. J. Cell Biol. 27: 137A.

Lee, D. L. (1974). Observation on the ultrastructure of a cephalic sense organ of the nematode *Mermis nigrescens*. J. Zool. Lond. 173: 247-250.

Li, J., Ashton, F.T., Gamble, H. R. and Schad, G. A. (2000a). Sensory neuroanatomy of a passively ingested nematode parasite, *Haemonchus contortus*: amphidial neurons of the first-stage larva. J. Comp. Neurol. 417: 299-314.

Li, J., Zhu, X., Ashton, F.T., Gamble, H. R. and Schad, G.A. (2001). Sensory neuroanatomy of a passively ingested nematode parasite, *Haemonchus contortus*: amphidial neurons of the third-stage larva. J. Parasitol. 87: 65-72.

Li, J., Zhu, X., Boston, R., Ashton, F.T., Gamble, H. R. and Schad, G.A. (2000b). Thermotaxis and thermosensory neurons in infective larvae of *Haemonchus contortus*, a passively ingested nematode parasite. J. Comp. Neurol. 424: 58-73.

Locke, M. (1994). Preservation and contrast without osmication or section staining. Microsc. Res. and Tech. 29: 1-10.

Nelson, H., Webster, J.M. and Burr, A.H. (1971). A redescription of the nematode *Oncholaimus vesicarius* (Wieser, 1959) and observations on the pigment spots of this species and of *Oncholaimus skawensis* Ditlevsen, 1921. Can. J. Zool. 49: 1193-1197.

Rees, G. (1950). Observation on the vertical migrations of the third-stage larva of *Haemonchus contortus* (Rud.) on experimental plots of Lolium perenne in relation to meteorological and micrometerological factors. Parasitology 40: 127-143.

Pepe, I. M. (1999). Rhodopsin and phototransduction. J. Photochem. Photobiol. 48: 1-10.

Pionar, G. O. and Hess, R. (1977). *Romanomermis culicivorax*: morphological evidence of transcuticular uptake. Exp. Parasitol. 42: 27-33.

Rutherford T. A., and Webster, J. M. (1974). Transcuticular uptake of glucose by the entomophilic nematode, *Mermis nigrescens*. J. Parasitol. 60: 804-808.

Siddiqui, A. and Viglierchio, D.R. (1970 a). Fine structure of photoreceptors in *Deontostoma californicum*. J. Nematol. 2: 274-276.

Siddiqui, A. and Viglierchio, D.R. (1970 b). Ultrastructure of photoreceptors in the marine nematode *Deontostoma californicum*. J. Ultrastruct. Res. 32: 558-571.

Strote, G., Bonow, I. and Attah, S. (1996). The ultrastructure of the anterior end of male *Onchocerca volvulus*: papillae, amphids, nerve ring and first indication of an excretory system in the adult filarial worm. Parasitology 113: 71-85.

Sulston, J. and Hodgkin, J. (1988). Methods. In: The Nematode *Caenorhabditis elegans*. Edited by W. B. Wood. pp. 587-606. Cold Spring Harbor Laboratory Press, New York.

Tchesunov, A. V. and Hope, W. D. (1997). *Thalassomermis megamphis* n. gen., n. sp. (Mermithidae: Nemata) from the Bathyal South Atlantic Ocean. J. Nematol. 4: 451-464.

Trett, M. W. and Lee, D. L. (1981). The cephalic sense organs of adult female *Hammerschmidtiella diesingi* (Nematoda: Oxyuroidea). J. Zool. 194: 41-52.

Van De Velde, M. C. and Coomans, A. (1988). Ultrastructure of the photoreceptor of *Diplolaimella* sp. (Nematoda). Tissue Cell 20: 421-429.

Vanfleteren, J. R. (1982). A monophyletic line of evolution? Ciliary induced photoreceptor membranes. In: Visual Cells in Evolution. Edited by J. A. Westfall. pp. 107-136. New York, Raven Press.

Ward, S., Thomson, N., White, J.G. and Brenner, S. (1975). Electron microscopical reconstruction of the anterior sensory anatomy of the nematode *Caenorhabditis elegans*. J. Comp. Neurol. 160: 313-337.

Wolken, J. J. (1977). *Euglena:* The photoreceptor system for phototaxis. J. Protozool. 24: 518-522.

Wolken, J. J. (1987). Light and Life Processes.Van Nostrand Reinhold Company, New York, pp.107-126.

Wright, K.A. (1983). Nematode chemosensilla: Form and function. J. Nematol. 15: 51-158.